A new akidnognathid synapsid specimen from the Permian of Cradock, South Africa and the revision of *Hewittia albanensis*

JUSTIN KYLE LLOYD and FRANCOIS DURAND

Lloyd, J.K. and Durand, F. 2025. A new akidnognathid synapsid specimen from the Permian of Cradock, South Africa and the revision of *Hewittia albanensis*. *Acta Palaeontologica Polonica* 70 (2): 339–355.

The main Karoo Basin of South Africa has yielded a treasure trove of fossil synapsids ranging from the middle Permian to the Early Jurassic, spanning approximately 80 Myr. *Hewittia albanensis* was first described by Brink (1959) based on AMG 4208 collected from the Chris Hani District Municipality (former Cradock District), Eastern Cape Province, South Africa. Since then, the taxon has been mostly ignored in published research. Here, we provide a redescription of *H. albanensis* based on a new specimen recovered from the Chris Hani District Municipality within rocks of the *Lystrosaurus maccaigi–Moschorhinus* Subzone of the *Daptocephalus* Assemblage Zone. We propose a new genus name for this species, *Cradognathus*, since *Hewittia* Brink, 1959, is preoccupied by *Hewittia* de Lessert, 1928, a crab spider from Congo. The position of *Cradognathus* within the Akidnognathidae, as well as its generic diagnosis, are revisited and discussed. The new specimen consists of an almost complete skull with some dorsoventral distortion. *Cradognathus* differs from other akidnognathids by the dental formula, a sharply pointed pterygoid transverse process, a median keel anterior to a short interpterygoid vacuity, and the presence of prominent lateral tuberosities at the ends of the ventromedial pterygoid flanges. We find that *Cradognathus* forms a clade with *Euchambersia*, *Cerdosuchoides*, and *Moschorhinus* within Akidnognathidae.

Key words: Therapsida, Therocephalia, Akidnognathidae, South Africa, Changhsingian, Permian.

Justin Kyle Lloyd [justinkl04@gmail.com; ORCID: https://orcid.org/0000-0003-2661-2497] and Francois Durand [fdurand@uj.ac.za; ORCID: https://orcid.org/0000-0003-2966-1163], Department of Zoology, University of Johannesburg, University Road and Kingsway Avenue, Aukland Park, Johannesburg, 2092, South Africa.

Received 3 July 2024, accepted 2 May 2025, published online 30 June 2025.

Introduction

Fossil synapsids are of particular interest in understanding the origin and evolution of mammals (Kemp 2005). Synapsids also provide vital information regarding adaptation, diversification, and succession, having survived several mass extinctions (Huttenlocker 2014; Grunert et al. 2019; Viglietti et al. 2021). Early synapsids were important parts of the first terrestrial vertebrate-dominated ecosystems that included carnivores, scavengers, insectivores, and abundant herbivores (Kemp 2005).

The synapsid fossils of the Main Karoo Basin of southern Africa provide the most complete evolutionary record of the origin of mammals from non-mammalian synapsids and enable us to trace the origin of mammalian characteristics within this evolutionary succession. Within the primarily carnivorous synapsid group Theriodontia, Therocephalia is widely considered to be the sister group of the Cynodontia (the group from which mammals arose, approximately 200 million years ago; Hopson and Barghusen 1986; Van Den Heever 1994; Rubidge and Sidor 2001; Huttenlocker 2009; Botha-Brink and Modesto 2011, Huttenlocker and Abdala 2015; Huttenlocker and Smith 2017; Liu and Abdala 2017, 2019, 2020, 2022; Grunert et al. 2019, Pusch et al. 2021, 2023; Sidor et al. 2021).

In conflict with this prevailing hypothesis of relations, several characteristics of derived therocephalians (Eutherocephalia) showing similarities to the palatal and braincase morphology of cynodonts suggest that Therocephalia could be paraphyletic with regards to Cynodontia. Pusch et al. (2024) most recently found this to be the case, with Cynodontia forming a sister-clade relationship with Eutherocephalia and basal therocephalians (Lycosuchidae, Scylacosauridae) falling outside this clade. Other authors previously recovered a paraphyletic Therocephalia, albeit with different topologies, such as finding cynodonts to form a sister-clade relationship with the whaitsiid *Theriognathus*

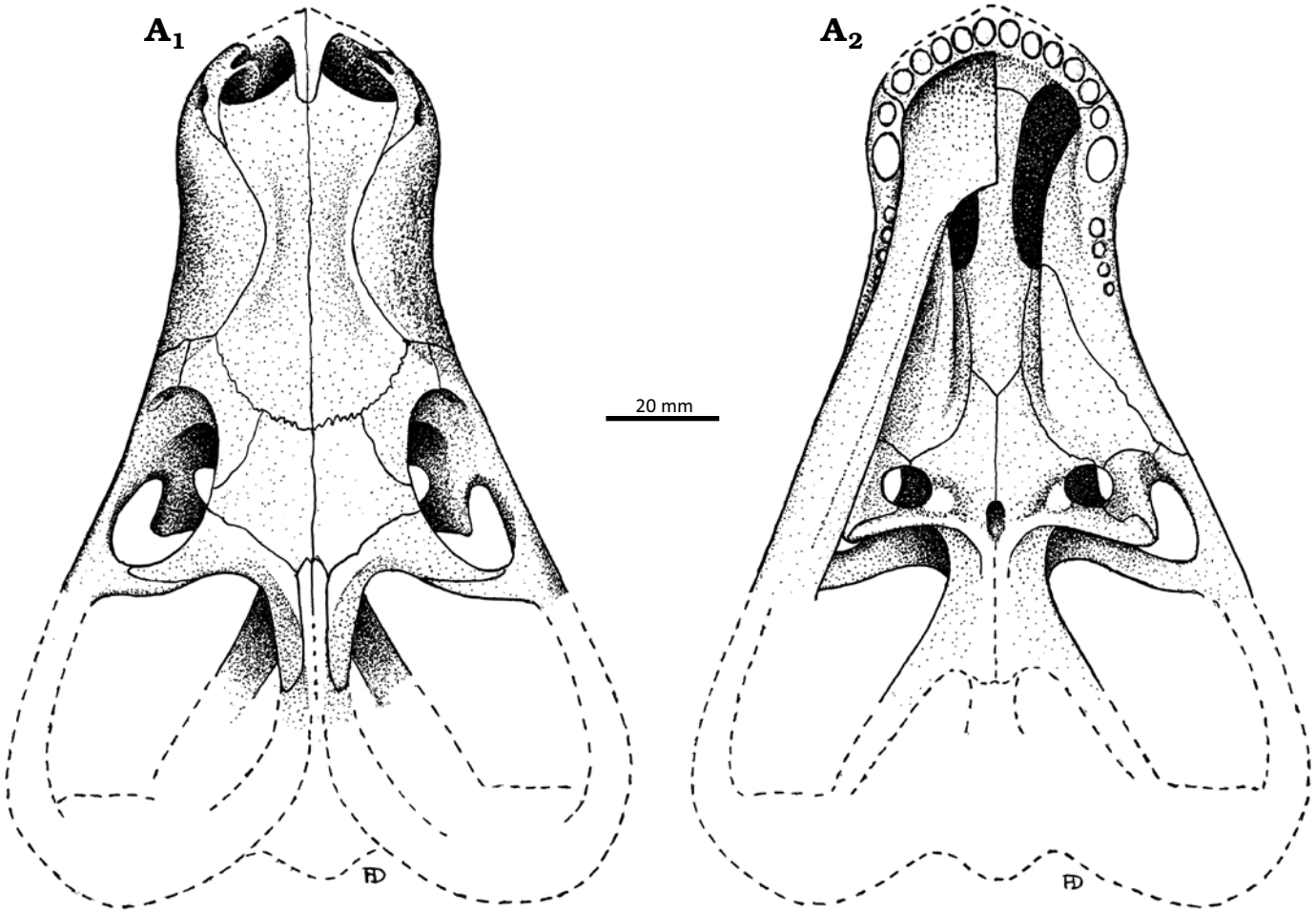

Fig. 1. The original illustrations of the akidnognathid synapsid "*Hewittia albanensis* Brink, 1959" holotype (AMG 4208), from originally upper *Cistecephalus* Zone and likely now the *Lystrosaurus maccaigi–Moschorhinus* Subzone of the upper Permian *Daptocephalus* Assemblage Zone, upper Changhsingian of the uppermost Permian (~253 to 252 Ma), Chris Hani (previously Cradock) District, South Africa. Specimen in dorsal (A_1) and ventral (A_2) views. Redrawn from the original drawings used in Brink (1986).

(Botha et al. 2007; Abdala 2007; originally proposed by Kemp 1972) or the baurioid *Microgomphodon* (Abdala et al. 2019).

Therocephalian fossils are known from the Permo-Triassic deposits of Russia, China, Africa, and Antarctica (Kemp 2005; Botha-Brink and Modesto 2011; Angielczyk and Kammerer 2018). Therocephalia diversified and reached its greatest species richness in the Permian but survived into the Triassic of Africa, Eurasia, and Antarctica, with various forms adapted for herbivory, insectivory, and carnivory. Therocephalians exhibit an array of mammal-like characteristics (Huttenlocker 2009, 2013; Huttenlocker and Sidor 2012; Huttenlocker and Abdala 2015) that, as mentioned above, may represent either convergence or ancestry relative to cynodonts. Within eutherocephalians, three major subclades are recognized: Akidnognathidae, Whaitsioidea (including Hofmeyriidae and Whaitsiidae), and the large and diverse group Baurioidea. Akidnognathidae, which include *Moschorhinus*, *Olivierosuchus*, *Promoschorhynchus,* and *Hewittia,* have been recovered as the earliest-diverging of these groups (Huttenlocker 2009), forming an evolutionary link between the more plesiomorphic scylacosaurid and lycosuchid therocephalians and the more derived whaitsiid and baurioid eutherocephalians.

The holotype of *Hewittia albanensis* is a partial skull with occluded partial lower jaw missing the portions posterior to the orbit (AMG 4208; Fig. 1). In 1993, a second more complete specimen attributed to *Hewittia albanensis* (CGP/1/2301) was recovered. CGP/1/2301 is an almost complete, albeit distorted and slightly crushed, skull (Fig. 2) and was used in this study to provide a redescription of this taxon. The new information obtained from describing its craniodental and mandibular anatomy indicates that *H. albanensis* is a valid taxon and permits us to propose a new genus name to replace the preoccupied *Hewittia* Brink, 1959, and to incorporate it into a phylogenetic analysis for the first time.

Nomenclatural acts.—This published work and the nomenclatural acts it contains have been registered in ZooBank: urn:lsid:zoobank.org:pub:3AE1F3FA-4FB4-4269-A1E9-D0CB92122262.

Institutional abbreviations.—AMG, Albany Museum, Grahamstown (since 2018 Makhanda), South Africa; BP, Evo-

lutionary Studies Institute, University of the Witwatersrand, Johannesburg (originally Bernard Price Institute for Palaeontology), South Africa; CGP, Council for Geoscience, Pretoria, South Africa; NMQR, National Museum, Bloemfontein, South Africa; SAM, Iziko South African Museum, Cape Town, South Africa; RC, Rubidge Collection, Graaff-Reinet, South Africa; USNM, National Museum of Natural History, Washington D.C., USA.

Other abbreviations.—c/C, lower/upper canine; i/I, lower/upper incisor; pc/PC, lower/upper postcanine; pC, upper precanine.

Material and methods

The specimen CGP/1/2301 (Fig. 2) is a nearly complete skull that is distorted transversely and compressed dorsoventrally that caused damage to the lateral wall of the braincase creating a crack across both epipterygoids. The right jugal is also almost entirely missing. Part of the lower jaw has been preserved. The left dentary bone and the right post dentary bones have been lost. The specimen was borrowed from the Council for Geoscience for this project.

The fossil was excavated from the grey mudstone at an exposure on the farm Lombardsrus (32°16'29"S, 25°52'25"E) and mechanically cleaned. An air hammer was used to remove most of the matrix from the skull in 1993.

The material that was used in this comparative study are: the type specimen of *Hewittia albanensis* (AMG 4208) and *Moschorhinus kitchingi* (BP/1/1713, BP/1/2205, NMQR 3658), *Promoschorhynchus platyrhinus* (BP/1/484, SAM-PK-K10014, RC 116), *Euchambersia mirabilis* (BP/1/384), *Olivierosuchus parringtoni* (BP/1/3849; NMQR3605, SAM-PK-K117), *Akidnognathus parvus* (SAM-PK-4201), *Cerdosuchoides brevidens* (CGS CM-86-778), *Theriognathus microps* (BP/1/512, BP/1/717, BP/1/747, RC211), and *Bauria cynops* (BP/1/1685, BP/1/3770).

Systematic palaeontology

Synapsida Osborn, 1903

Therocephalia Broom, 1903

Akidnognathidae Nopcsa, 1923

Genus *Cradognathus* nov.

ZoobankLSID:urn:lsid:zoobank.org:act:4BCE5BCE-0979-46B2-A985-B2432F70888D.

Etymology: Combination of Crado, from the name of the nearest town (Cradock, South Africa) to the type locality at the time of collection and Ancient Greek *gnathus*, jaw.

Type species: *Hewittia albanensis* Brink, 1959; monotypic. Exact type locality unknown, Chris Hani District Municipality, South Africa; Changhsingian, upper Permian.

Remarks.—Replacement name for *Hewittia* Brink, 1959, which is preoccupied by a genus of crab spider (*Hewittia* de Lessert, 1928).

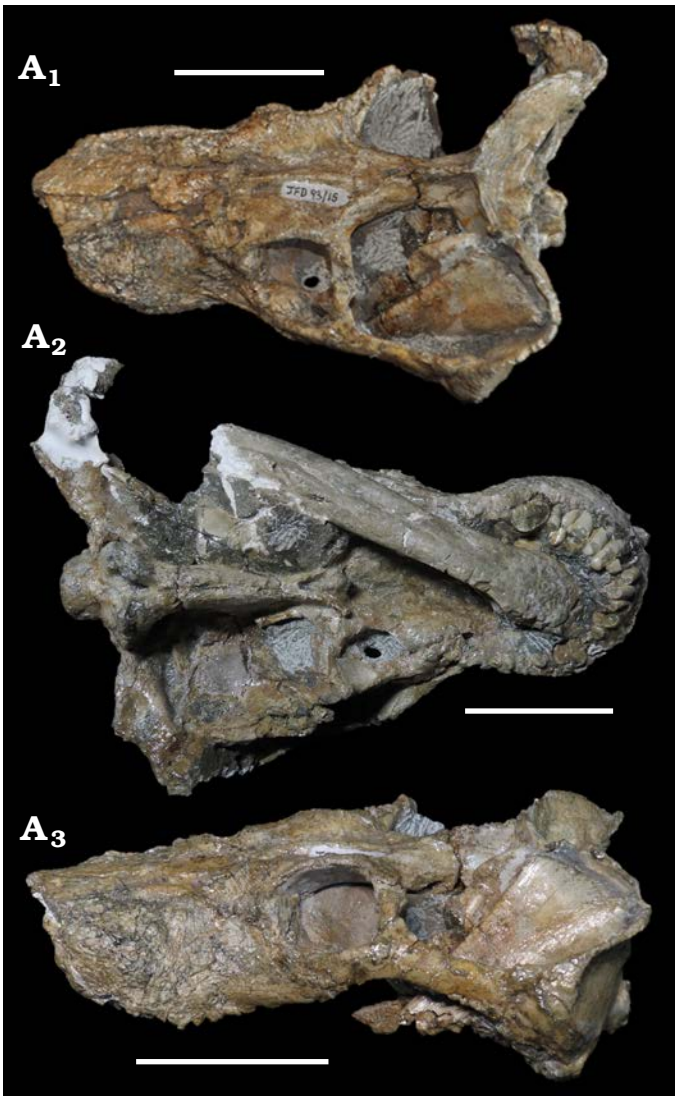

Fig. 2. Photographs of the akidnognathid synapsid *Cradognathus albanensis* (Brink, 1959), CGP/1/2301, from the *Lystrosaurus maccaigi–Moschorhinus* Subzone of the upper Permian *Daptocephalus* Assemblage Zone, upper Changhsingian of the uppermost Permian (~253 to 252 Ma), Chris Hani (previously Cradock) District, South Africa. Specimen in dorsal (A_1), ventral (A_2), and left lateral (A_3) views. Scale bars 50 mm.

Diagnosis.—As for the monotypic type species.

Cradognathus albanensis (Brink, 1959)

Figs. 1, 2, 4–11.

Holotype: AMG 4208, partial skull with occluded partial lower jaw that misses the portions posterior to the orbit. Erroneously reported as No. 4206 by Brink (1959).

Type locality: The exact locality of the type specimen is unknown apart from being from the Chris Hani District Municipality (former Cradock District), South Africa.

Type horizon: Elandsberg Member, Balfour Formation, Beaufort Group, upper Permian. Originally reported as from *Cistecephalus* Zone by Brink (1959) based on the accepted biostratigraphical zonation at the time, which has since been updated. The actual biozone of origin

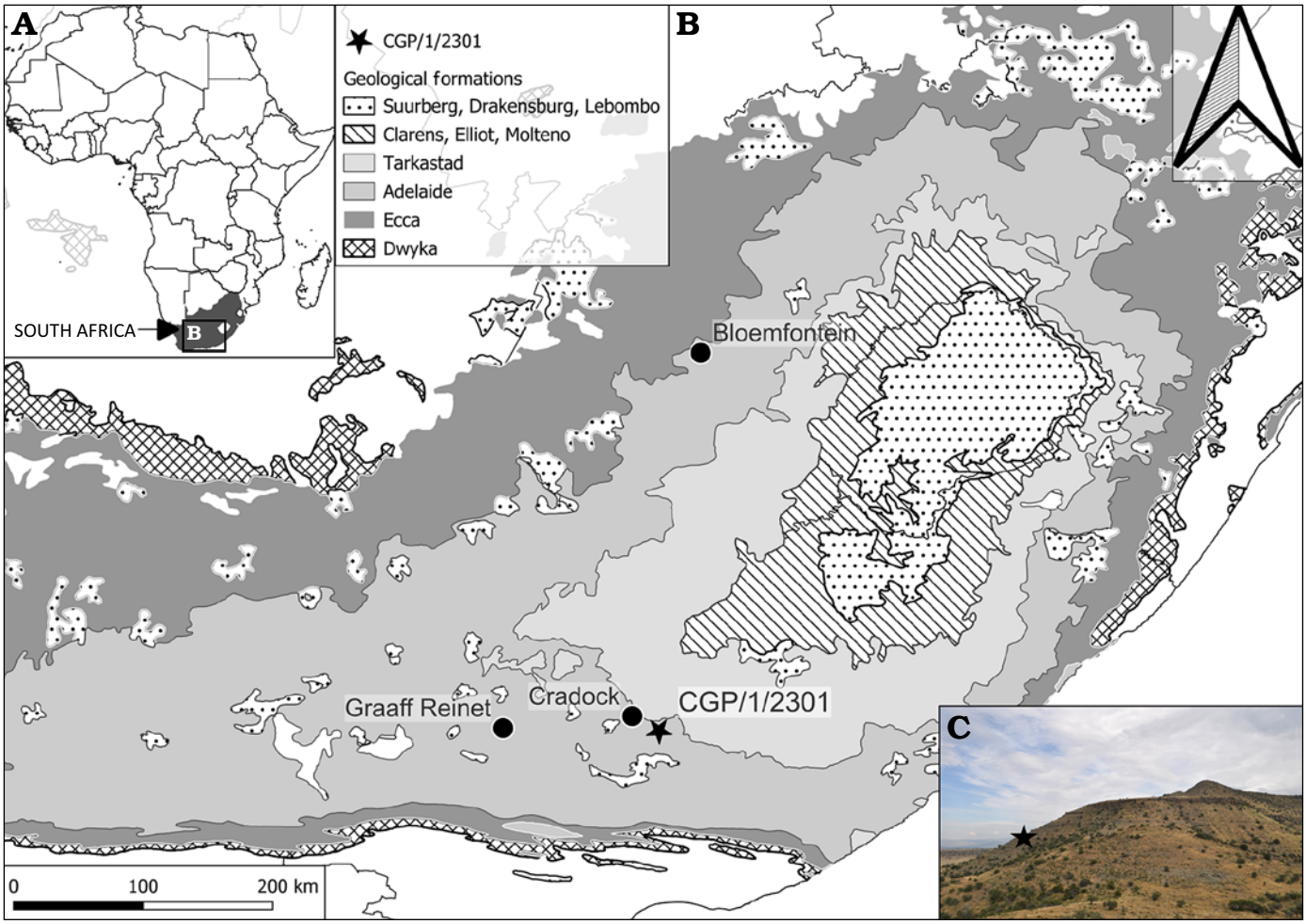

Fig. 3. **A**. ap showing location of the study area. **B**. Geological map of the Farm Lombardsrust area in the Karoo Supergroup, where the specimen CGP/1/2301 of *Cradognathus albanensis* (Brink, 1959) was found, *Lystrosaurus maccaigi–Moschorhinus* Subzone of the upper Permian *Daptocephalus* Assemblage Zone, upper Changhsingian of the latest Permian (~253 to 252 Ma), Chris Hani (previously Cradock) District, South Africa. **C**. Photograph of the locality.

is most likely the upper Permian *Daptocephalus* Assemblage Zone, *Lystrosaurus maccaigi–Moschorhinus* Subzone, based on what is primarily exposed in this area (Viglietti 2020).

Material.—CGP/1/2301, almost complete skull and with occluded partial lower jaw, collected at 32°16'29.863"S, 25°52'23.987"E (Fig. 3) on the Farm Gannavlakte 494, known as Lombardsrust, Cradock, Chris Hani District Municipality of the Eastern Cape Province in South Africa. The locality in which it was found falls within the *Lystrosaurus maccaigi–Moschorhinus* Subzone of the upper Permian *Daptocephalus* Assemblage Zone of the Balfour Formation, just below the Permo-Triassic boundary (Viglietti 2020; Smith et al. 2020).

Diagnosis.—The skull has a low, elongated snout with slender, elongated dentaries, a thickened symphysial region, and a backward-sloping chin. The dental formula is I5-pC1-C1-PC4 (upper) and i3-c1-pc4 (lower). The palate is similar to a species of *Moschorhinus*, although more delicate, with big, deep-seated suborbital vacuities in prominent, sharply pointed triangular transverse processes. A secondary hard palate is absent, but the presence of choanal cristae on the medial surface of the palatines suggests the presence of a soft palate. A prominent diamond-shaped tuberosity, instead of a median keel, seen in other akidnognathids, occurs in front of the short triangular interpterygoid vacuity that differs in shape from the elongated slit-like interpterygoid vacuity seen in other akidnognathids. This median tuberosity is flanked by the crescent-shaped ventromedial flanges of the pterygoids that end in prominent lateral tuberosities adjacent to the suborbital vacuities. Apomorphies include three, rather than four, lower incisors, a diastema between the main canine and first upper postcanine, a distinct mastoid process, and the apparent absence of a posterior apophysis of the epipterygoid.

Description.—The snout of CGP/1/ 2301 resembles that described for the akidnognathid *Promoschorhynchus* (Mendrez 1974; Huttenlocker et al. 2011) and the whaitsiid *Theriognathus* (Huttenlocker and Abdala 2015), whereas the snout of the akidnognathids *Moschorhinus* (Boonstra 1934; Durand 1989, 1991) and *Euchambersia* (Liu and Abdala 2022) are much shorter, broader, and more robust than that of the aforementioned taxa, with a large maxillary fossa taking up much of the lateral surface of the snout in *Euchambersia*

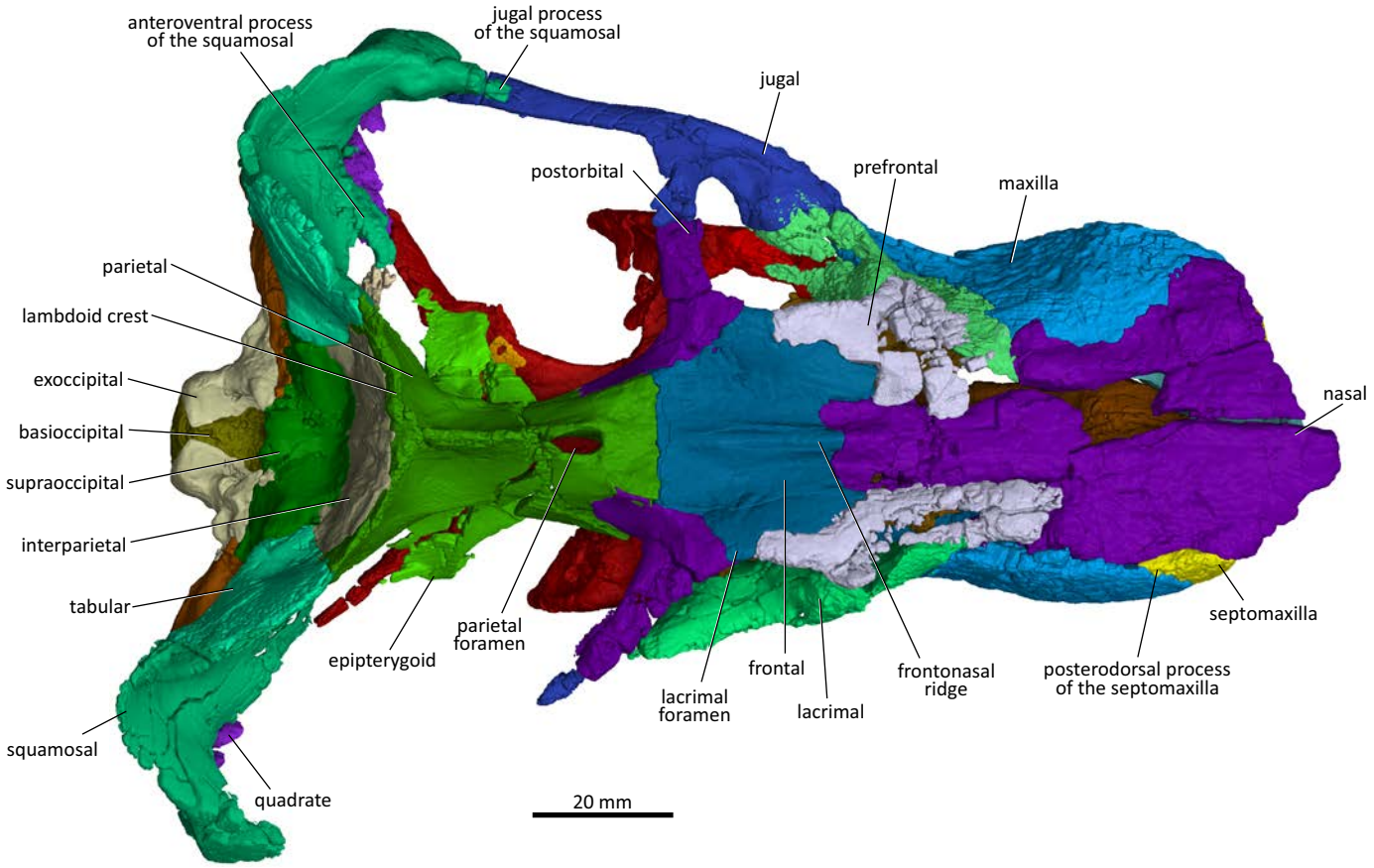

Fig. 4. 3D reconstruction of the akidnognathid synapsid *Cradognathus albanensis* (Brink, 1959), CGP/1/2301, *Lystrosaurus maccaigi–Moschorhinus* Subzone of the upper Permian *Daptocephalus* Assemblage Zone, upper Changhsingian of the uppermost Permian (~253 to 252 Ma), Chris Hani (previously Cradock) District, South Africa. Specimen in dorsal view.

(Benoit et al. 2017; Liu and Abdala 2022). There is a slight lateral constriction in the snout of CGP/1/2301 and AMG 4208, deepening posteriorly from behind the canine to the lacrimal region where it reaches its maximum extent (Figs. 1, 2, 4, 5), similar to that seen in *Promoschorhynchus* (Mendrez 1974), *Jiufengia* (Liu and Abdala 2019), *Olivierosuchus* (Botha-Brink and Modesto 201; Gigliotti et al. 2023), and *Theriognathus* (Huttenlocker and Abdala 2015). Due to damage to the anteriormost portion of the snout, only the left septomaxilla is well preserved (Figs. 4–6). It has a broad plate overlaying the premaxilla and a distinct posterodorsal process that forms a wedge between the nasal and maxilla dorsally. The maxillo-septomaxillary fossa lies on the septomaxilla-maxilla contact. The premaxilla articulates with the surrounding bones by means of three processes: the internarial process of the premaxilla, the maxillary process of the premaxilla, and the vomerine process of the premaxilla. The maxillary process of the premaxilla extends laterally, below the septomaxilla, and continues posterolaterally where it meets the anterior border of the maxilla just anterior to the precanine (Fig. 6). The maxillary foramen is situated on this suture. The vomerine process extends posteriorly along the roof of the buccal cavity, where it meets the vomer at the level of the anterior border of the internal nasal choanae. Each premaxilla houses five laterally compressed incisors and the alveolar margin shows a slight upturning at the point of the fourth incisor. This upturning appears in some other akidnognathids, including *Jiufengia* (Liu and Abdala 2019), *Moschorhinus* (Durand 1989, 1991), and *Olivierosuchus* (Gigliotti et al. 2023), but is absent in *Shiguaignathus* (Liu and Abdala 2017) as well as non-akidnognathids like the basal therocephalian *Lycosuchus* (Pusch et al. 2020) or the cynodont *Galesaurus* (Pusch et al. 2019). Different specimens of *Euchambersia* and *Promoschorhynchus* vary in this character, with the *Promoschorhynchus* specimen SAM-PK-K10014 (Huttenlocker and Abdala 2015) being the only specimen with the upturning present. *Euchambersia* differs in morphology between the South African species (*Euchambersia mirabilis*; see Benoit et al. 2017) showing no upturning and the Chinese specimen (*Euchambersia liuyudongi*; see Liu and Abdala 2022) with the upturning present.

The maxilla (Figs. 4–7) is a wide, broad bone with a dorsal lamina that projects highly dorsally creating a narrowing of the nasals midway along the length and articulates with the septomaxilla, the premaxilla, the prefrontal, and the lacrimal on the snout. The maxilla articulates by means of the posterior jugal process with the ventral aspect of the lacrimal and the anterior margin of the jugal anteroventral to the orbit. The external surface of the maxilla is finely rugose in lateral view. In ventral view, the maxilla folds over, creating

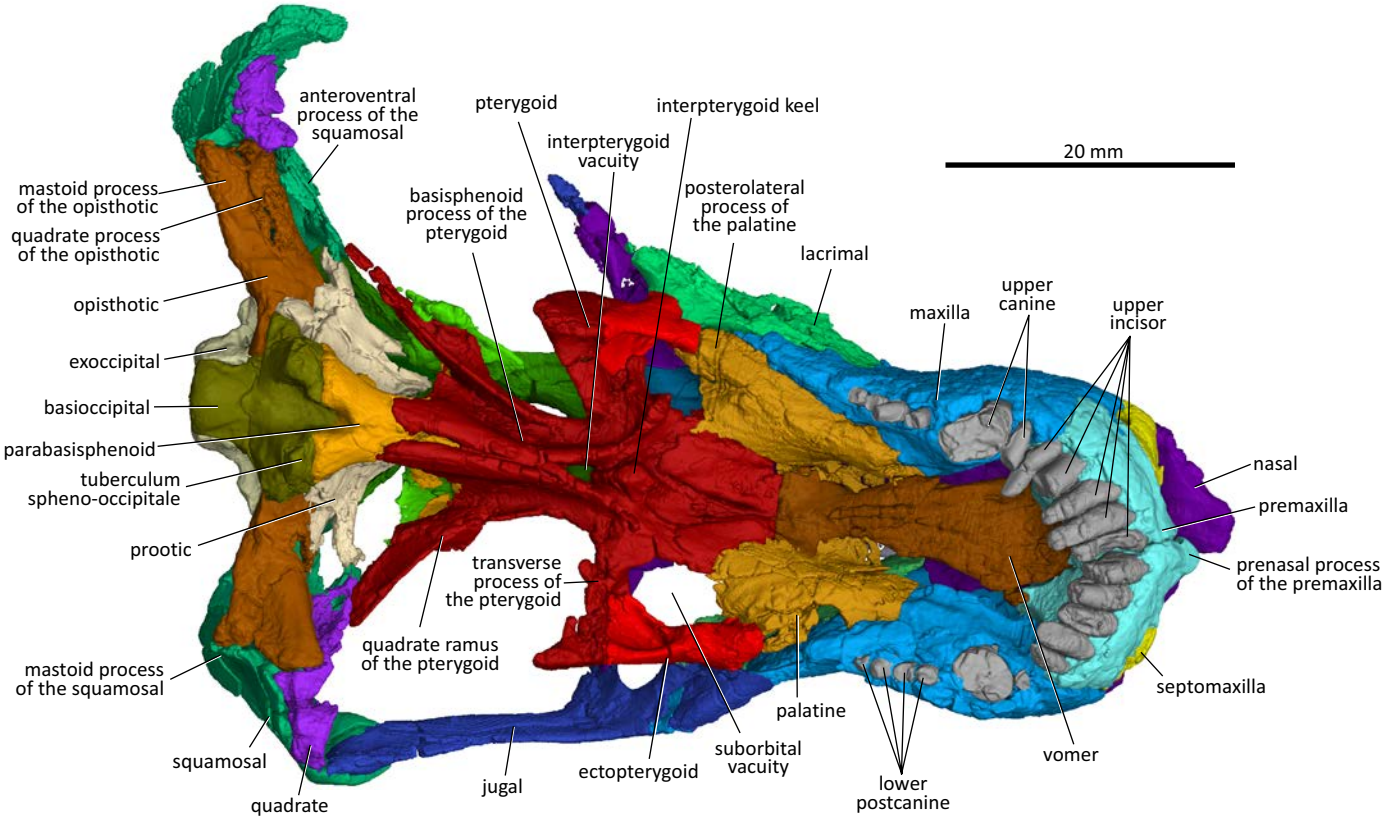

Fig. 5. 3D reconstruction of the akidnognathid synapsid *Cradognathus albanensis* (Brink, 1959), CGP/1/2301, *Lystrosaurus maccaigi–Moschorhinus* Subzone of the upper Permian *Daptocephalus* Assemblage Zone, upper Changhsingian of the uppermost Permian (~253 to 252 Ma), Chris Hani (previously Cradock) District, South Africa. Specimen in ventral view.

a strong and robust alveolar margin. The maxilla-palatine foramen lies on the suture between the palatine and maxilla, at the level of the second postcanine. Each maxilla bears one incisiform precanine, one large canine, and four small postcanine teeth. This condition differs from that described for the akidnognathid *Olivierosuchus*, which has only three postcanine teeth (Botha-Brink and Modesto 2011; Gigliotti et al. 2023).

Despite fracturing and weathering of the snout, it is evident that the lateral surface of the snout of CGP/1/2301 is rugose, similar to that of other akidnognathids such as *Moschorhinus* and *Olivierosuchus*, but differs in that respect from the snouts described for non-akidnognathid eutherocephalians such as *Bauria* and *Theriognathus* that have smooth surfaces (Brink 1963; Botha-Brink and Modesto 2011). CT scans had to be used to reconstruct the lingual surface of the maxilla due to the lower jaw obscuring the view. The choanal crest (crista choanalis) is a blunt ridge, similar to that of *Moschorhinus* (Durand 1989, 1991), rather than sharp as that of *Olivierosuchus* and *Theriognathus* (Brink 1965; Botha-Brink and Modesto 2011). This ridge can be seen beginning at the anterior extent of the palatine and extending posteriorly until the anterior margin of the suborbital vacuity (Fig. 5) in the akidnognathids *Olivierosuchus* and *Shiguaignathus*, as well as in *Lycosuchus* (Liu and Abdala 2017; Pusch et al. 2020; Gigliotti et al. 2023). The secondary palate remains open, lacking a vomeromaxillary contact, similar to that of other akidnognathids (Botha-Brink and Modesto 2011). The primary palate of CGP/1/2301 is similar to that of *Promoschorhynchus* and *Olivierosuchus.* The anterior portion of the vomer is expanded at the contact with the premaxilla before narrowing along its length and expanding again at its contact with the fused pterygoids and the palatines. Along the midsagittal length on the ventral surface of the vomer, there is a ridge called the ventromedial crest of the vomer, which is a common feature in akidnognathids (Mendrez 1974; Durand 1989, 1991; Liu and Abdala 2017; Gigliotti et al. 2023).

The nasal bones (Figs. 4–6) are elongated and form the dorsomedial part of the nasal cavity and the central part of the dorsal surface of the snout (Fig. 2). The dorsal surface of the nasals is extensively damaged in CGP/1/2301, but despite being compressed, giving the nasals a sunken appearance (Brink 1959), they are in a relatively good condition in AMG 4208. As in other therocephalians, the nasals form an almost V-shaped suture pointing towards the occiput with the anterior margin of the frontal bones anterior to the level of the orbits. The lateral margin of the nasal contacts the prefrontal, maxilla, and premaxilla. A distinct sagittal frontonasal ridge runs along the contact between the frontals and nasals (Fig. 4). This is a common feature described by Durand (1989, 1991) in *Moschorhinus*, Botha-Brink and Modesto (2011) and Gigliotti et al. (2023) in *Olivierosuchus*, and Huttenlocker and Abdala (2015) in *Theriognathus*.

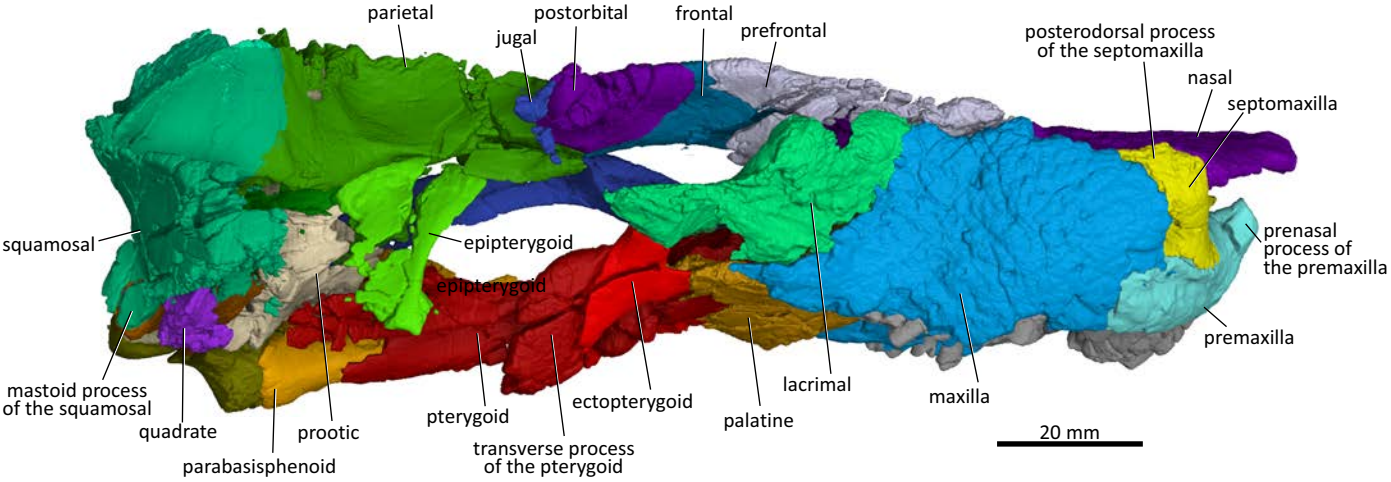

Fig. 6. 3D reconstruction of the akidnognathid synapsid *Cradognathus albanensis* (Brink, 1959), CGP/1/2301, *Lystrosaurus maccaigi–Moschorhinus* Subzone of the upper Permian *Daptocephalus* Assemblage Zone, upper Changhsingian of the uppermost Permian (~253 to 252 Ma), Chris Hani (Previously Cradock) District, South Africa. Specimen in lateral view.

There is a noticeable lateral constriction in the nasal bones of CGP/1/2301 and AMG 4208, where it sutures with the maxilla. This is a common feature shared with other akidnognathids such as *Olivierosuchus*, *Promoschorhynchus*, and the whaitsiid *Theriognathus*, although it is more pronounced in CGP/1/2301.

The frontals of both specimens are preserved (Figs. 1, 2, 4, 6) and resemble those of other akidnognathids (Mendrez 1974; Durand 1989; Botha-Brink and Modesto 2011; Gigliotti et al. 2023). The frontal contacts the nasal anteromedially, the prefrontal anterolaterally, the postorbital posterolaterally, and the parietal posteriorly. The interlacing transverse frontal-parietal suture is situated further anteriorly in CGP/1/2301 than that described by Brink (1959) for AMG 4208. The frontonasal ridge extends from the frontal to the nasal. It is most pronounced on the frontal and tapers anteriorly on the nasal. The frontonasal ridge of CGP/1/2301 is narrower than that of *Moschorhinus*.

The parietal (Figs. 1, 2, 4, 6, 7) forms the roof of the braincase. As in other akidnognathids, the parietal has a sharp sagittal crest that splits posteriorly to form the two lambdoid crests posterolaterally. The parietal contacts the frontal anteriorly, the postorbital anterolaterally, the epipterygoid and prootic ventrolaterally, and the squamosal and tabular posterolaterally. The parietal of CGP/1/2301 houses a pronounced spindle-shaped pineal canal similar in size to that of *Akidnognathus* (SAM-PK-4201), *Moschorhinus* (BP/1/4636) ,and *Theriognathus* (Huttenlocker and Abdala 2015). The presence of the pineal foramen is common in most akidnognathids but is missing in *Euchambersia* (Liu and Abdala 2022) and possibly in *Jiufengia* (Liu and Abdala 2019).

The orbits of CGP/1/2301 and AMG 4208 are distorted due to vertical compression. The anteroventral quarter of the rim of the orbit is formed by the lacrimal, while the jugal forms the posteroventral quarter of the orbit, with the dorsal process of the jugal forming the ventral half of the postorbital bar. The postorbital forms the posterodorsal corner, while the prefrontal forms the anterodorsal corner of the orbit. The frontal forms a thin wedge between the prefrontal and postorbital on the dorsal margin of the orbit (Figs. 2, 4, 6, 7).

The prefrontal articulates (Figs. 4, 6, 7) with the maxilla, nasal, lacrimal, and frontal. The anterior process of the prefrontal of CGP/1/2301 is relatively shorter than those of *Moschorhinus* and *Theriognathus* and resembles that of *Olivierosuchus* (Gigliotti et al. 2023). The anterior margin of the prefrontal of CGP/1/2301 articulates with the maxilla anteriorly running anteromedially while its anteromedial surface articulates with the nasal. This margin runs anteromedially here and in *Moschorhinus*, but anterolaterally in *Olivierosuchus* (Botha-Brink and Modesto 2011; Gigliotti et al. 2023) and *Theriognathus* (Huttenlocker and Abdala 2015). The lateroventral margin of the prefrontal articulates with the anterodorsal margin of the lacrimal, while its posteromedial margin articulates with the anterolateral margin of the frontal (Figs. 4, 6).

The postorbital (Figs. 4, 6, 7) of CGP/1/2301 is more delicate than that of *Theriognathus* (Huttenlocker and Abdala 2015) and *Moschorhinus* (Durand 1989, 1991) and resembles that of *Olivierosuchus* (Huttenlocker and Abdala 2015). The posterolateral process of the postorbital forms the dorsal part of the postorbital bar that joins up with the dorsal process of the jugal to form a complete postorbital bar, which is typical for akidnognathids, differentiating them from some later Triassic baurioids where the postorbital bar is incomplete (Brink 1963; Botha-Brink and Modesto 2011; Huttenlocker and Botha-Brink 2013). The postorbital of the akidnognathid *Jiufengia* projects further ventrolaterally to a point where it contributes to the suborbital bar (Liu and Abdala 2019). In CGP/1/2301, the postorbital does not reach the level of the suborbital bar.

The lacrimal (Figs. 4–7) of CGP/1/2301 is completely occluded from contacting the nasal by the prefrontal, which is

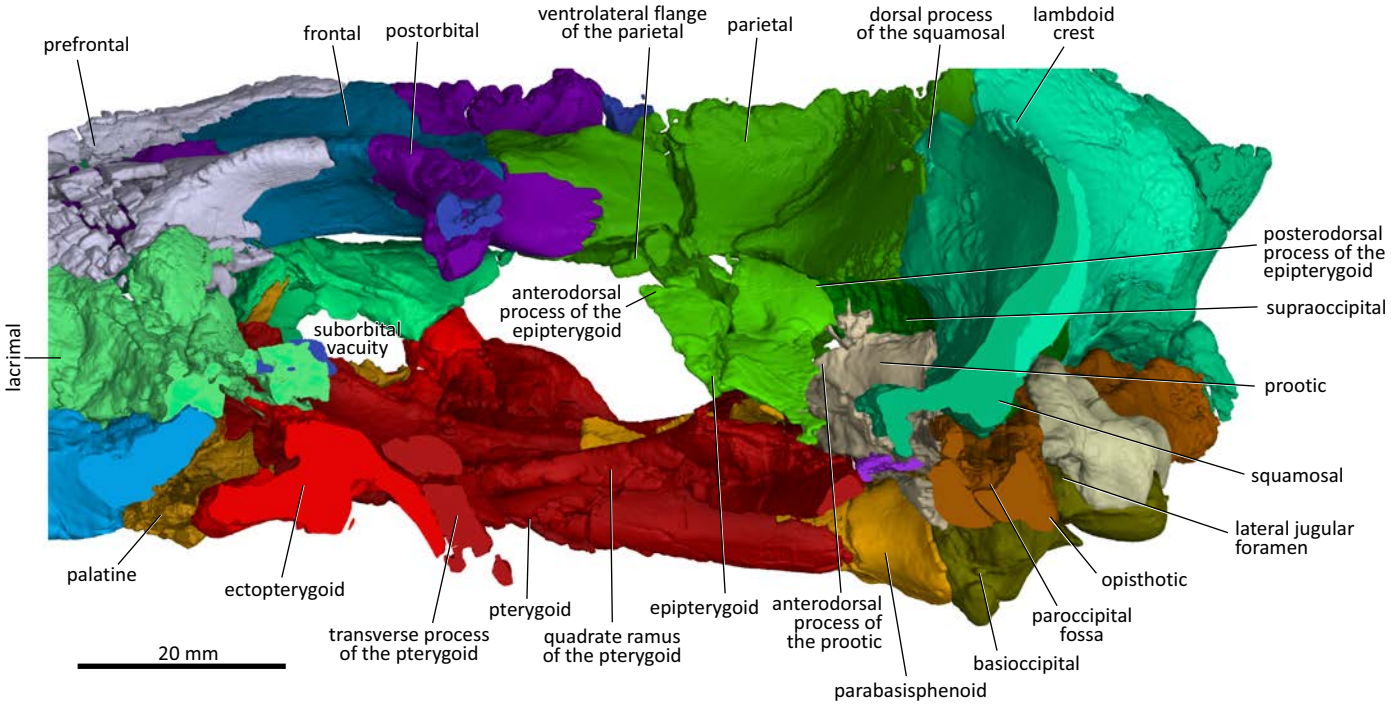

Fig. 7. 3D reconstruction of the akidnognathid synapsid *Cradognathus albanensis* (Brink, 1959), CGP/1/2301, *Lystrosaurus maccaigi–Moschorhinus* Subzone of the upper Permian *Daptocephalus* Assemblage Zone, upper Changhsingian of the uppermost Permian (~253 to 252 Ma), Chris Hani (previously Cradock) District, South Africa. Braincase in lateral view, with the subtemporal and suborbital bars removed.

common amongst therocephalians (Huttenlocker and Abdala 2015). The anterior margin of the lacrimal is difficult to distinguish in AMG 4208, leading to the erroneous interpretation of Brink (1959), where a contact between the lacrimal and nasal is described (Fig. 1). The dorsal margin of the lacrimal contacts the prefrontal, together forming the anterior wall of the orbit. The suture between the lacrimal and prefrontal continues anterior to the orbit on the lateral wall of the snout, curving dorsally (Fig. 6). The anterior margin of the lacrimal sutures with the maxilla. The lacrimal contacts the jugal posterolaterally, forming the orbit's ventral rim (Figs. 4, 6). The lacrimal is excluded from contact with the nasals by the prefrontal, which is a common feature of therocephalians apart from *Lycideops* (Sigurdsen et al. 2012; Pusch et al. 2020). The lacrimal duct penetrates the lacrimal and is situated just inside the anteroventral rim of the orbit.

The vomer (Fig. 5) forms the medial part of the roof of the mouth and is flanked on either side by the choanae. The broad anterior margin of the vomer forms a curved suture with the premaxillae at the level of the anterior border of the internal nasal choanae. The interchoanal part of the vomer tapers posteriorly, creating the posteromedial curvature of the medial wall of the choanae. The vomer spreads out posterior to the choanae into lateral concave surfaces that are confluent with the choanae anteriorly and continues on the palatines with which the vomer sutures posteriorly. A similar morphology is seen in *Olivierosuchus* (Gigliotti et al. 2023) and *Promoschorhynchus* (Mendrez 1974). A narrow ventromedial crest occurs on the posterior half of the vomer, which is similar to those found in *Promoschorhynchus*, *Olivierosuchus*, *Shiguaignathus*, and *Theriognathus* (Mendrez 1974; Botha-Brink and Modesto 2011; Huttenlocker and Abdala 2015; Liu and Abdala 2017; Gigliotti et al. 2023), but is not present in *Jiufengia* (Liu and Abdala 2019) (Fig. 5).

The three jugal processes extend anteriorly, dorsally, and posteriorly (Figs. 4–6). The dorsal process forms the ventral part of the postorbital bar, while the anterior process joins up with the posterior process of the maxilla to form the lower rim of the orbit. The subtemporal ramus of the jugal extends posteriorly to join with the anteroventral ramus of the squamosal to form the subtemporal bar, which is more robust in *Moschorhinus* than in CGP/1/2301. In *Moschorhinus,* the anterior process appears extremely short relative to its thickness and the subtemporal ramus is dorsoventrally thin anteriorly and thickens posteriorly.

The ectopterygoid forms the lateral rim of the suborbital vacuity. It articulates with the palatine anterior to the suborbital vacuity and the transverse process of the pterygoid posterior to the suborbital vacuity (Fig. 5). The suborbital vacuities are rounded, unlike the laterally expanded vacuities in *Moschorhinus* and *Promoschorhynchus* (Mendrez 1974; Durand 1989, 1991). *Olivierosuchus* and *Shiguaignathus* also shows more rounded suborbital vacuities (Botha-Brink and Modesto 2011; Liu and Abdala 2017; Gigliotti et al. 2023). *Jiufengia* has exceptionally large suborbital vacuities compared to the other akidnognathids (Liu and Abdala 2017: fig. 3).

The palatine's lateral margin contacts the maxilla's medial margin in ventral view (Fig. 5). The palatine forms the anterior wall of the suborbital vacuity and articulates with the ec-

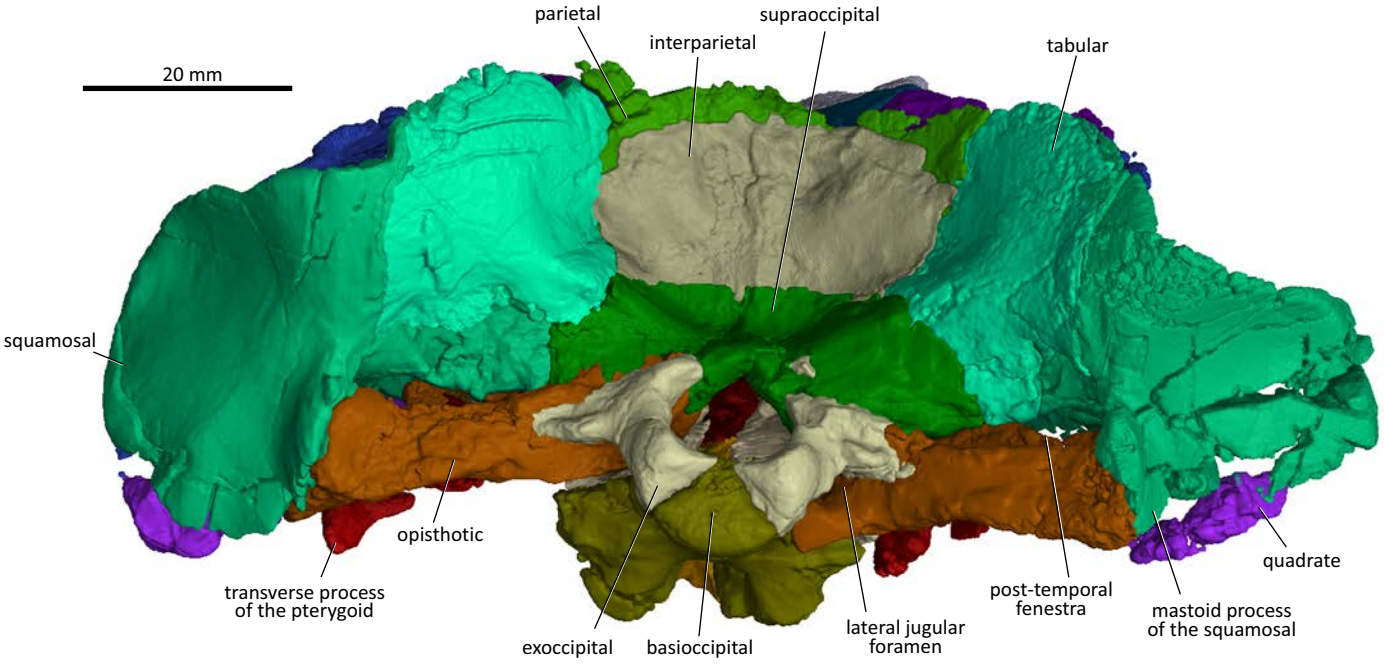

Fig. 8. 3D reconstruction of the akidnognathid synapsid *Cradognathus albanensis* (Brink, 1959), CGP/1/2301, *Lystrosaurus maccaigi–Moschorhinus* Subzone of the upper Permian *Daptocephalus* Assemblage Zone, upper Changhsingian of the uppermost Permian (~253 to 252 Ma), Chris Hani (previously Cradock) District, South Africa. Specimen in posterior view.

topterygoid posterolaterally, the anterior margin of the pterygoid posteromedially and with the vomer medially. Although less pronounced than in *Moschorhinus*, a distinct crista choanalis runs along the medial surface of the palatine that forms the lateral wall of the choana in both AMG 4208 and CGP/1/2301. This crista choanalis possibly marks the place of attachment of the secondary soft palate (Brink 1959; Maier et al. 1996). The deep palatine gutters, which connect the posterior part of the choanae and the suborbital vacuities, run across the medial aspect of the palatines dorsal to the cristae choanalis. This differs from the condition in the phylogenetically uncertain eutherocephalian *Ichibengops* (Huttenlocker and Abdala 2015), whaitsiid *Theriognathus* (Huttenlocker and Abdala 2015), and baurioid *Bauria* (Brink 1963), where there is a single concavity posterior to the choanae involving the palatines and vomers on both sides. In contrast, there are two separate gutters in CGP/1/2301, *Olivierosuchus* (Gigliotti et al. 2023), *Moschorhinus* (Durand 1989, 1991), and *Shiguaignathus* (Liu and Abdala 2017). Medial ridges that originate on the vomer anteriorly extend over the medial border of the palatine and flatten out on the pterygoid as it approaches the suborbital vacuity. These ridges form the medial wall of these palatine gutters.

The pterygoids are complex bones that form a major part of the basicranium (Figs. 4, 5, 7, 8). The transverse process of the pterygoid lines the posteromedial rim of the deeply excavated suborbital vacuity and joins the ectopterygoid to form the prominent sharp-pointed triangular pterygoid process in ventral view. As in other akidnognathids such as *Olivierosuchus*, *Promoschorhynchus*, *Shiguaignathus*, and *Moschorhinus*, there is a short and deep median bulge, keel, or crest in front of the interpterygoid vacuity that divides the anterior part of the interpterygoid vacuity in CGP/1/2301. Whereas the interpterygoid keel is spindle-shaped or narrow in the other akidnognathids, it is a diamond-shaped tuberosity in CGP/1/2301. The ventromedian keel is missing in the akidnognathids *Jiufengia* (Liu and Abdala 2019) and *Euchambersia* (Liu and Abdala 2022). The ventromedial flanges of the pterygoids are prominent features that form the central and most ventral part of the basicranium. These ridges flare anterolaterally and extend onto the transverse processes of the pterygoids, similar to those of *Olivierosuchus*, *Promoschorhynchus*, and *Moschorhinus*. There are prominent tuberosities on the lateral ends of these anterolateral ridges similar to those of *Olivierosuchus* and *Promoschorhynchus*. The above ridges are described in *Shiguaignathus* but there is no indication of them ending in tuberosities. The interpterygoid vacuity of CGP/1/2301 seems to be relatively shorter than those of *Promoschorhynchus*, *Moschorhinus*, and *Akidnognathus* (Haughton 1918; Mendrez 1974; Durand 1989). Still, it does extend, albeit in a very constricted fashion, between the two ventromedial ridges of the pterygoids up to the thin spindle-shaped parasphenoid keel that is situated between the posterior parts of the ventromedial ridges of the posteromedial part of the pterygoids. The posterior end of the quadrate ramus of the pterygoid contacts the quadrate, opisthotic, and squamosal posteriorly. The foot of the epipterygoid sutures with the dorsal surface of the pterygoid's quadrate ramus.

The braincase of CGP/1/2301 is formed by the parietal dorsally, the supraoccipital posterodorsally, the basioccipital and parabasisphenoid ventrally, the prootic and opist-

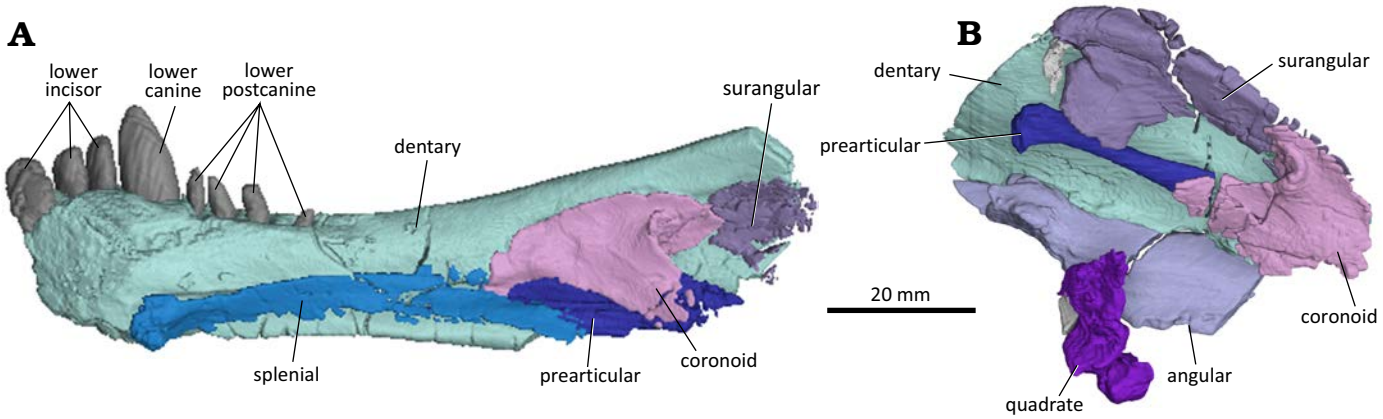

Fig. 9. 3D reconstruction of the akidnognathid synapsid *Cradognathus albanensis* (Brink, 1959), CGP/1/2301, *Lystrosaurus maccaigi–Moschorhinus* Subzone of the upper Permian *Daptocephalus* Assemblage Zone, upper Changhsingian of the uppermost Permian (~253 to 252 Ma), Chris Hani (previously Cradock) District, South Africa. Right (**A**) and left (**B**) lower jaw in medial view.

hotic posterolaterally, and the dorsal part of the epipterygoid laterally (Figs. 4–9). It resembles other akidnognathids in that the posterior part of the braincase is ossified while the lateral part consists of bony elements and non-ossified tissue (Barry 1965; Durand 1989). There were no indications of the presence of an orbitosphenoid; however, using more high-powered scanning methods might reveal this delicate structure.

The parasphenoid and basisphenoid are fused to form the parabasisphenoid complex, which articulates with the basioccipital posteriorly and the pterygoid anteriorly (Fig. 5). A thin parasphenoid keel is lodged between the ventromedial flanges of the pterygoid, however the ventral portion that would have protruded has been broken off, leaving little to describe externally.

The occipital area resembles that of other akidnognathids and comprises the supraoccipital, exoccipitals, basioccipital, interparietal, parietal, tabulars, squamosals, opisthotics, and the quadrate-quadratojugal complexes (Fig. 8).

The occipital condyle comprises the basioccipital flanked by posteroventral extensions of the exoccipitals, and also forms the posteroventral part of the basicranium (Figs. 4, 5, 8). The exoccipitals form the greater part of the walls of the foramen magnum, with the basioccipital and supraoccipital elements present as thin strips of bone separating the exoccipitals on the floor and the roof of the foramen magnum, respectively (Fig. 8). The foramen for the hypoglossal nerve (N XII) passes through the exoccipital and can be seen on the ventromedial surface of the foramen magnum. The supraoccipital sutures with the interparietal dorsally, the tabulars dorsolaterally and the opisthotic bones ventrolaterally (Fig. 8). The basioccipital sutures anteriorly with the parabasisphenoid complex, with which it forms the two spheno-occipital tuberculae, seen in ventral view (Fig. 5).

A low medial ridge originates on the occipital surface of the parietal, extends ventrally over the interparietal and ends ventrally against the dorsal margin of the supraoccipital (Fig. 8). The deep depressions on both sides of this low ridge, housed in the interparietal, were probably for the attachment of epaxial neck muscles. The interparietal sutures with the parietal dorsally, the tabulars laterally, and the supraoccipital ventrally.

The tabulars articulate with the parietal dorsomedially, the interparietal medially, the supraoccipital and opisthotic ventromedially, and the squamosal laterally to ventrolaterally (Fig. 8). The anterior surface of the tabular covers the posterior surface of the squamosal and contributes, together with the squamosal, to the lambdoidal crest.

In lateral view (Figs. 6, 7), the epipterygoid of CGP/1/2301 has an hourglass shape similar to that of *Moschorhinus* (Durand 1989, 1991) and *Euchambersia* (Barry 1965; Liu and Abdala 2022). The epipterygoid contacts the parietal dorsally and covers its dorsal rim with a short descending ventrolateral flange. The epipterygoid contacts the quadrate process of the pterygoid ventrally and the supraoccipital posterodorsally. The epipterygoids of CGP/1/2301 were crushed during compression. Still, there seems to be no evidence of a posterior apophysis and no contact between the epipterygoid and the anterodorsal process of the prootic, differing from that in *Moschorhinus* (Durand 1989, 1991), *Promoschorhynchus* (Mendrez 1974; Huttenlocker et al. 2011), *Jiufengia* (Liu and Abdala 2019), and *Theriognathus* (Huttenlocker and Abdala 2015).

The opisthotic of CGP/1/2301 is a robust and thick bone that juts transversely out from the basicranium medially to the jaw hinge laterally (Figs. 5, 8). The medial edge of the opisthotic articulates with the exoccipital and basioccipital. The jugular foramen is situated between the opisthotic and the exoccipital (Figs. 5, 8). The short posterodorsal process of the opisthotic contacts the exoccipital medially, the supraoccipital dorsomedially, the tabular dorsally, and laterally with the intermediate process of the squamosal inside the post-temporal fenestra (Fig. 8). The dorsal surface of the opisthotic splits into two flanges, the anterodorsal flange and the posteroventral flange with a gutter-like elongated hollow, with the paroccipital fossa in between, ventral to the post-temporal fenestra. This resembles the condition described for the opisthotics of *Promoschorhynchus* (Mendrez 1974) and *Moschorhinus*

(Durand 1989, 1991). The posteroventral flange of the opisthotic (the mastoid process of the opisthotic) articulates with the mastoid process of the squamosal laterally. The anterodorsal flange of the opisthotic joins the posterovental process of the prootic medially to complete the anterior wall of the paroccipital fossa (Fig. 8). The opisthotic forms the posteroventral border of the fenestra ovalis (Fig. 5).

The squamosal of CGP/1/2301 is a large bony element that forms a significant part of the lateral aspects of the posterior part of the skull. It sutures with the jugal anteriorly via the zygomatic process, the parietal, interparietal, supraoccipital, and prootic medially, the opisthotic, the quadrate ramus of the pterygoid, quadratojugal, and quadrate ventrally, and the tabular posteriorly (Figs. 4, 5, 7, 8). The jugal process of the squamosal forms the posterior half of the jugal arch. Three processes extend medially from the squamosal: the dorsal, intermediate and anteroventral processes. The dorsal process of the squamosal sutures with the parietal and interparietal on the side wall of the braincase, while the posterior surface of this portion is covered by the tabulars (Figs. 4, 7, 8). The intermediate process of the squamosal articulates with the interparietal, supraoccipital, and prootic on the lateral aspect of the braincase (Fig. 7). In occipital view, the squamosal articulates with the ventrolateral margin of the tabulars and posterodorsal process of the opisthotic (Fig. 8). The anteroventral process of the squamosal contacts the central process of the prootic to form the anteroventral margin of the post-temporal fenestra and the anterior bar enclosing the pterygo-paroccipital foramen. The mastoid process of the squamosal contacts the quadrate-quadratojugal complex ventrolaterally. However, the exact nature of this contact could not be determined in CGP/1/2301 because of the extensive damage to both sides in this area (Fig. 2). The mastoid process of the squamosal encapsulates the lateral aspect of the opisthotic medial to the quadrate-quadratojugal contact (Figs. 2, 5, 8). The stapes is missing in CGP/1/2301.

The dentary (Fig. 9) is a long element that forms a major part of the lower jaw and houses the lower dentition. The dentary is relatively slender, with a relatively straight ventral margin and with a thickened symphysial region where it supports the single canine and the incisors. It is not possible to determine the fusion of this region with the anterior position of the right dentary being missing. The anterior end of the dentary slopes upwards lacking a distinctive chin and the anterolateral surface is slightly rugose. Along the lateral surface, there is a distinctive groove or lateral sulcus. There is no diastema present between the canine and the first postcanine. On the left side, the posterior end of the of the dentary is preserved and shows a coronoid process which narrows slightly anteriorly before being broken off. On the dorsal surface, medial to the postcanines, there is a shelf present leaving the postcanines more exposed on the medial surface than on the lateral surface. Along the medial surface, there is an anteroposteriorly-running gutter housing the splenial anteriorly and the prearticular posteriorly.

The dentary is slender with a thickened symphysial region, which is common in akidnognathids and *Lycosuchus* (Botha-Brink and Modesto 2011; Pusch et al. 2020; Gigliotti et al. 2023). Although it is not possible to determine the level of fusion of the symphysis here with complete certainty, it was likely unfused as in other therocephalians (Botha-Brink and Modesto 2011; Pusch et al. 2020; Gigliotti et al. 2023). The anterior end slopes gently as in *Lycosuchus*, *Olivierosuchus*, and *Promoschorhynchus* and lacks the strong distinctive chin seen in *Moschorhinus* and *Jiufengia* (Durand 1989; Botha-Brink and Modesto 2011; Liu and Abdala 2019; Pusch et al. 2020; Gigliotti et al. 2023). The ventral margin is not as strongly curved as in *Theriognathus* and is rather straight, like in *Olivierosuchus* and *Promoschorhynchus* (Mendrez 1974; Botha-Brink and Modesto 2011; Huttenlocker and Abdala 2015; Gigliotti et al. 2023). A similar shelf on the dorsomedial surface along the row of postcanines is seen in *Lycosuchus* (Pusch et al. 2020).

The angular (Fig. 9) is largely missing on both sides.

The surangular (Fig. 9) although damaged, is present and the general morphology could be determined. It is a transversely narrow bone that sits on the medial surface of the dentary. It is narrow, but as robust and as thick as the dentary. It is present high relative to the dentary and can be seen above the dorsal extent of the coronoid process. In dorsal view it has a slightly convex dorsal border and in ventral view it has a lightly concave ventral border. The anterior and posterior ends show a ventrally projecting flange exaggerating the concavity of the ventral border. The posterior end shows a second flange that projects posteriorly forming a slight notch between the two posterior flanges.

The position of the surangular is much higher than that of other therocephalians but this may just be due to distortion rather than the actual morphology. Although the *Olivierosuchus* specimen NMQR 4605 also shows this bone quite high (Botha-Brink and Modesto 2011), in the type specimen BP/1/3849 it is much lower (Gigliotti et al. 2023: fig. 13B). The curving morphology of the surangular, displaying a convex dorsal margin is also seen in other therapsids (Huttenlocker and Abdala 2015; Huttenlocker and Sidor 2020; Pusch et al. 2020; Gigliotti et al. 2023).

The splenial (Fig. 9) is a long, thin element that runs along a medial groove on the medial surface of the dentary being completely obscured laterally. Only the splenial on the right side is preserved along with the dentary. It begins at the ventromedial extent of the dentary at the ventral point of the mandibular symphysis and ends just posterior to the mid-length of the dentary ventral to the prearticular. It likely contributed to the ventral limit of the mandibular symphysis.

The morphology and position of the splenial within the medial or Meckelian groove of the dentary conforms to that seen in other therocephalians and cynodonts (Huttenlocker and Sidor 2020; Gigliotti et al. 2023). The contribution of the splenial to the ventral extent of the symphysis is common in therapsids (Van Den Heever 1994; Huttenlocker and Sidor 2020; Pusch et al. 2020, 2023; Gigliotti et al. 2023).

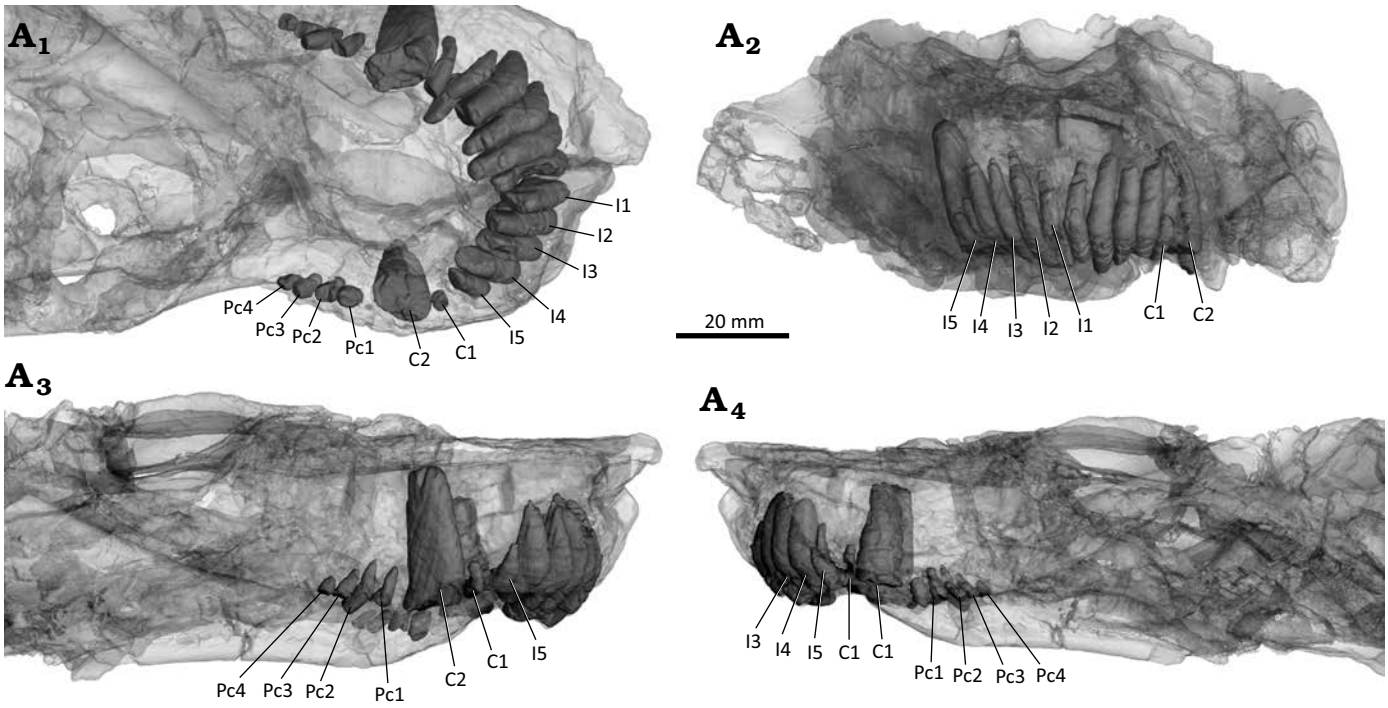

Fig. 10. 3D reconstruction of the akidnognathid synapsid *Cradognathus albanensis* (Brink, 1959), CGP/1/2301, *Lystrosaurus maccaigi–Moschorhinus* Subzone of the upper Permian *Daptocephalus* Assemblage Zone, upper Changhsingian of the uppermost Permian (~253 to 252 Ma), Chris Hani (Previously Cradock) District, South Africa. Dentition of the upper jaw in ventral (A_1), anterior (A_2), left (A_3) and right (A_4) lateral views.

The coronoid (Fig. 9) is a thin, roughly triangular element covering the anterior portion of the surangular, the anterior portion of the angular, the anterior portion of the prearticular, and the anterodorsal extent of the angular. The coronoid is only visible on the left side using the ct scans, as it is completely obscured by the dentary laterally. The lateral surface is smooth and slight convex. The coronoid is proportionally larger here and in *Olivierosuchus* (Gigliotti et al. 2023) than in *Lycosuchus* (Pusch et al. 2020).

The prearticular (Fig. 9) is a rod-shaped bone that is posterodorsally to anteroventrally orientated. It lies medial to the coronoid process of the dentary, posterolateral to the coronoid, ventral to the surangular, and dorsal to the angular. It is wider dorsoventrally than mediolaterally. It is narrowest midlength and expands anteriorly and posteriorly with posterior end forming a club-like end with a slight medial process.

The prearticular forms the ventral margin of the mandibular fenestra in other therapsids, but this area is completely covered laterally by the dentary in this taxon (Botha-Brink and Modesto 2011; Huttenlocker and Sidor 2020; Gigliotti et al. 2023).

The upper dentition (Fig. 10) is housed by the premaxilla and the maxilla and is largely preserved; however there is some damage, with the precanine missing on the left side. There are five incisors, one small precanine, one large canine, and four postcanines. The incisors are conically shaped, strongly recurved, and laterally compressed on either premaxilla. Most of the incisors are similar in size, with only a slight reduction from I1 to I4, but with I5 being significantly smaller than I4. The two upper canines are broken off at the point where they exit the jaw with the root intact with the remains showing the canines would be significantly larger than the precanine, the postcanines, and the incisors. The postcanines are small like those of most Akidnognathidae. All the upper postcanines are broken off at the point where they appear from the maxilla but can clearly be seen to be almost half the size of the incisors. There are no clear serrations or surface textures on what remains of the dentition and no indications of replacement activity. The number of postcanines differs slightly between most akidnognathids, including *Olivierosuchus* and *Moschorhinus* with three postcanines (Durand 1991; Gigliotti et al. 2023), *Promoschorhynchus* with five or six postcanines (Mendrez 1974), *Shiguaignathus* with eight postcanines (Liu and Abdala 2017), and *Euchambersia* that lacks postcanines (Benoit et al. 2017; Liu and Abdala 2022). *Jiufengia* appears to be the only identified akidnognathid that also displays four postcanines (Liu and Abdala 2017).

The lower dentition (Fig. 11) is supported entirely by the dentary and consists of three incisors, one large canine, and four postcanines. The three incisors are about half the size of the canine and much larger than the postcanines. The large lower canine being significantly larger than both the incisors and the postcanines. There are four lower postcanines in the dentary. The first three postcanines are approximately the same size but the fourth is barely visible extruding from the dentary. The lower postcanines are reduced in size and number with there being only four present here, less than the five in *Olivierosuchus* (Gigliotti et al. 2023) and the

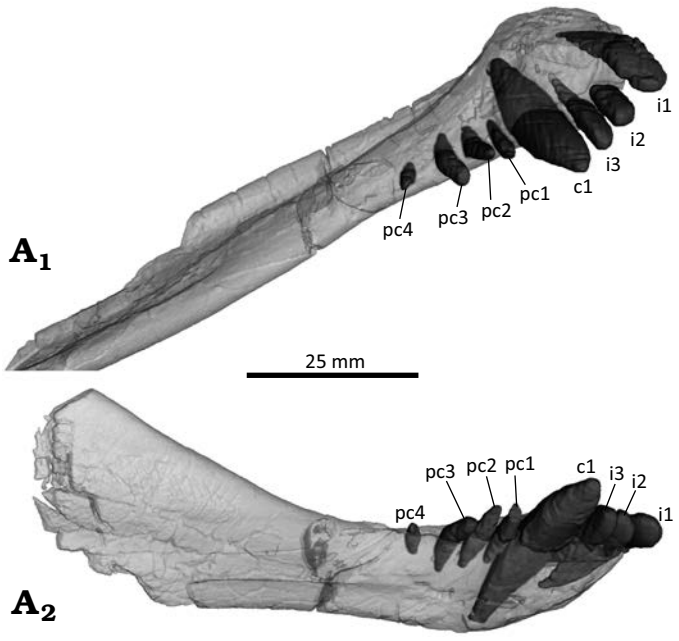

Fig. 11. 3D reconstruction of the akidnognathid synapsid *Cradognathus albanensis* (Brink, 1959), CGP/1/2301, *Lystrosaurus maccaigi–Moschorhinus* Subzone of the upper Permian *Daptocephalus* Assemblage Zone, upper Changhsingian of the uppermost Permian (~253 to 252 Ma), Chris Hani (previously Cradock) District, South Africa. Right mandible showing the lower dentition in dorsal (A_1) and lateral (A_2) views.

six in *Promoschorhynchus* (Mendrez 1974). There are no serrations or other surface textures on any of the lower teeth and no indications of replacement teeth present. The number of the lower incisors is less than in *Olivierosuchus* with four (Gigliotti et al. 2023), but the same as in the lycosuchid *Lycosuchus* (Pusch et al. 2020). The lower incisors appear thicker and more robust than in *Olivierosuchus* (Gigliotti et al. 2023: fig. 13).

Stratigraphic and geographic range.—Changhsingian, upper Permian; Chris Hani District Municipality (former Cradock District), South Africa.

Phylogenetic analysis

To ascertain the phylogenetic position of *Cradognathus albanensis* within the Akidnognathidae, this taxon was coded into the data set of the recent phylogenetic analysis of therocephalian relationships by Liu and Abdala (2022). The data matrix comprises 62 taxa and 129 discrete characters. AMG 4208 and CGP/1/2301 were used as a combined coding for *Cradognathus albanensis*, and the states were added to the analysis following the same methods. The coding for character 56, the presence of a posterior apophysis of the epipterygoid, was coded as present in *Olivierosuchus* by Liu and Abdala (2022). This was corrected based on descriptions of *Olivierosuchus* (Botha-Brink and Modesto 2011; Gigliotti et al. 2023) and personal observations. A heuristic search was done using PAUP v.4.0a (build 159) (Swofford 2002) using maximum parsimony with a random addition sequence with 1000 replicates and the tree bisection reconnection (TBR) branch-swapping algorithm. All characters were treated as unordered and given equal weight. Multistate taxa were considered as polymorphic. Gorgonopsia was set as the outgroup (Liu and Abdala 2022).

The parsimony analysis resulted in 14850 most parsimonious trees with a tree length of 461 (retention index = 0.7331, consistency index = 0.0.4273). The results of the analysis are represented as a 50% majority-rule consensus tree (Fig. 12) with the values at each node representing the bootstrap values for each clade and a strict consensus tree (see SOM, Supplementary Online Material available at http://app.pan.pl/SOM/app70-Lloyd_Durand_SOM.pdf). The majority rule consensus tree displays a monophyletic Akidnognathidae (bootstrap value of 94.55) with a largely pectinate topology with one taxa splitting off from the group at each step. *Annatherapsidus* as the most basal member followed by the two Chinese taxa: *Shiguaignathus* and *Jiufengia*. It then shows a split off by the unnamed akidnognathid USNM PAL 412421 followed by *Akidnognathus*. Next, we see the well-established *Olivierosuchus–Promoschorhynchus* (bootstrap value of 100) clade split off, followed by *Cradognathus*, which forms the sister taxon to the clade comprising *Cerdosuchoides*, *Moschorhinus*, and the two *Euchambersia* species. The latter is resolved in a polytomy at the apex of the tree only with the two *Euchambersia* species forming a clade.

Discussion

Huttenlocker (2013) diagnosed Akidnognathidae based on the following characteristics: the presence of a frontonasal crest, the buccally convex alveolar margin of the maxillary postcanines, the absence of a canine-postcanine diastema, a thickened dentary symphysis, and a palatine fossa for the tip of the mandibular canine. Huttenlocker (2009) included other characteristics in identifying akidnognathids, such as a septomaxilla that overlaps the premaxilla, enlarged, anterior-facing external nares, and an anteriorly expanded vomer (Huttenlocker 2009).

CGP/1/2301 conforms to all these identifiers, confirming its identification as an akidnognathid. It has a prominent frontonasal crest extending along the midline from the parietal-frontal suture over the frontal that continues anteriorly on the midline of the posterior part of the nasals. The buccal surface of the maxillary alveolar margin is convex, particularly medial to the canine, but also extends posteriorly, flanking the postcanines. There is no diastema between the canine and postcanines on the maxilla. The symphysis of the dentary is robust, and a large palatine fossa is present for the mandibular canine. The vomer is widely expanded anteriorly. The external nares are enlarged and anteriorly facing, separated by the remnants of the septomaxilla.

Fig. 12. 50% majority consensus tree depicting the phylogenetic position of *Cradognathus albanensis* within the Akidnognathidae. Numbers at the nodes represent the bootstrap values.

Comparison of *Cradognathus* with other akidnognathid eutherocephalians

CGP/1/2301 and *Akidnognathus* share several characteristics, such as incisors that are larger than the precanines and postcanines. There is a rounded suture present between the vomer and the premaxilla. The vomer possesses a posterior median keel. The interpterygoid vacuity is triangular in shape. Both have snouts that are broader than high, with a medial frontonasal ridge and anterior-facing external nares. The postorbitals are thin. Differences between CGP/1/2301 and *Akidnognathus* include seven postcanine teeth on the maxilla in *Akidnognathus* compared to the four postcanines in CGP/1/2301. The premaxilla of CGP/1/2301 extends further posteriorly. The snout and nasals of *Akidnognathus* are not constricted, as is the case in CGP/1/2301. *Akidnognathus* also differs from CGP/1/2301 in that it does not have an interpterygoid keel (the ventromedian keel of Huttenlocker 2013) or ventromedial flanges of the pterygoids (ventrointermediate crests of Huttenlocker 2013).

Unfortunately, the single specimen of the monototypic type species of *Cerdosuchus* has been lost. The only evidence that remains of *Cerdosuchus* is the descriptions of

Broom (1936) and Brink (1988). CGP/1/2301 resembles *Cerdosuchus* and shares several characteristics: the rugose maxilla, delicate postorbital, slender and long jugal, and relatively large pineal foramen. Differences include an extra postcanine and smaller precanines than those of CGP/1/2301 (Broom 1936; Brink 1986). Unfortunately, little is known of the palate and braincase of *Cerdosuchus*.

Cerdosuchoides also shares several characteristics with CGP/1/2301 but differs in that *Cerdosuchoides* has only three postcanines. The palate of *Cerdosuchoides* lacks the interpterygoid keel and the tuberosities at the ends of the ventromedial flanges of the pterygoids, that are characteristic of CGP/1/2301.

CGP/1/2301 shares several characteristics with *Moschorhinus* and, in many respects, looks like a slimmer, more gracile version of *Moschorhinus*. Characteristics that are shared include a low, broad snout, reduction of the number of postcanines, lateral compression of the incisors, hourglass-shaped epipterygoid, the frontonasal ridge, the keel in front of the interpterygoid vacuity and pronounced ventromedial flanges of the pterygoids. Differences between *Moschorhinus* and CGP/1/2301 include: the snout of *Moschorhinus* lacks the lateral constriction posterior to the level of the canines seen in CGP/1/2301 and other akidnognathids, the frontonasal crest of *Moschorhinus* is broader and resembles a low rounded ridge rather than the narrower, sharper crest of CGP/1/2301. CGP/1/2301 lacks the parasagittal furrows on the posterior part of the frontal anterior to the frontal-parietal suture. The interpterygoid keel has an elongated spindle shape in *Moschorhinus*, whereas CGP/1/2301 has a diamond-shaped interpterygoid keel. The vomer of CGP/1/2301 has a ventromedial keel, common in akidnognathids, whereas it splits into two ridges in *Moschorhinus*. The ventromedial flanges of the pterygoids of *Moschorhinus* are smooth compared to the ridges on those of CGP/1/2301. The cristae choanales of CGP/1/2301 are less prominent than those of *Moschorhinus.* The interpterygoid vacuity of CGP/1/2301 is short and triangular, whereas it is an elongated slit in *Moschorhinus*. The posteroventral process of the epipterygoid of *Moschorhinus* is elongated posteriorly, covers most of the posterior part of the quadrate process of the pterygoid and contacts the anteroventral process of the squamosal and the central process of the prootic. In contrast, the epipterygoid only contacts the quadrate process of the pterygoid in CGP/1/2301. The posterior apophysis, characteristic of *Moschorhinus*, is not present in CGP/1/2301, nor does the epipterygoid of CGP/1/2301 suture with the prootic.

Based on the descriptions and observations of all the akidnognathids, *Olivierosuchus* and *Promoschorhynchus* seem to be most similar to CGP/1/2301. This however differs from the results of the phylogenetic analysis. The characteristics they have in common include a delicate skull compared to *Moschorhinus*, and the lateral constriction in the snout, with the accompanying dorsomedial expansion of the maxilla and the narrowing of the nasals posteriorly (Brink 1965, Botha-Brink and Modesto 2011). All show a pronounced frontonasal ridge and parietal foramen. The ventromedial flanges of the pterygoids end laterally with pronounced ridges or tuberosities (Brink 1965). Whereas *Promoschorhynchus* and CGP/1/2301 have a similar size, shape, and detailed skull morphology, *Olivierosuchus* is smaller and more delicate and has a narrower snout, a more prominent crista choanalis, a narrower interpterygoid keel and a sharper frontonasal ridge.

In addition to all the characteristics mentioned above that CGP/1/2301 and *Promoschorhynchus* have in common, they both have a maxilla that contributes largely to the relatively slender suborbital bar, triangular interpterygoid vacuities, sharp-pointed transverse processes of the pterygoid and a short, thin parasphenoid keel.

Despite all the similarities between CGP/1/2301 and *Promoschorhynchus*, there are several differences. The crista choanalis is sharp-ridged in *Promoschorhynchus,* whereas it is subtle and less easily discernible in CGP/1/2301. The suture between the premaxilla and vomer is more crescent-shaped in CGP/1/2301 than in *Promoschorhynchus*. The basisphenoid processes of the pterygoid are robust, rounded, and elongated in CGP/1/2301 compared to their flat, short, and angular shape in *Promoschorhynchus*. The interpterygoid vacuity is broader in *Promoschorhynchus* than in CGP/1/2301. A diamond-shaped tuberosity in CGP/1/2301 represents the interpterygoid keel, whereas *Promoschorhynchus* is spindle-shaped like other akidnognathids and *Moschorhinus*. The ventromedial flanges of the pterygoids bend laterally in a crescent shape that ends in tuberosities in CGP/1/2301. In contrast, in *Promoschorhynchu*s, the ventromedial flanges of the pterygoids jut out as pronounced slightly anterolaterally projecting straight ridges with tuberosities. The epipterygoids of *Promoschorhynchus* are thicker than that of CGP/1/2301 and it has a posterior apophysis similar to that of *Moschorhinus*, whereas CGP/1/2301 has none. There is the possibility that the fracturing and compression CGP/1/2301 were subjected to could have destroyed the delicate posterior apophysis if it were present, however. The anteroventral and posteroventral processes of the epipterygoid of *Promoschorhynchus* are more prominent and extend further anteriorly and posteriorly, respectively, than that of CGP/1/2301. The dental formula of CGP/1/2301 and *Promoschorhynchus* differs. *Promoschorhynchus* has four dentary incisors, one more than CGP/1/2301. There are four dentary postcanines in CGP/1/2301, while there are six in *Promoschorhynchus*. *Promoschorhynchus* may have four to six maxillary postcanines, whereas CGP/1/2301 has four.

CGP/1/2301 represents, in all probability, the same taxon as AMG 4208, the holotype of *H. albanensis* as described by Brink (1959). Despite the damage and distortion CGP/1/2301 and AMG 4208 were subjected to, they are virtually identical. Some of their unique characteristics include the constriction of the snout posterior to the canine, which is more pronounced than that of other akidnognathids, causing a lateral narrowing of the nasals. They also have crescent-shaped ventromedial flanges of the pterygoids that end laterally with pronounced tuberosities, a short triangular, instead

of an elongated slit-like, interpterygoid vacuity, and a diamond-shaped interpterygoid tuberosity instead of an elongated keel as in other akidnognathids. Both specimens also possess sharp triangular transverse processes with deeply excavated suborbital vacuities.

The original description of AMG 4208 (Brink 1959) contains several inconsistencies that were cleared up after examination of CGP/1/2301. Brink (1959) describes four lower incisors in AMG 4208; however, after examining the specimen, it was agreed by the authors that it had only three lower incisors that match those of CGP/1/2301. Brink (1959) describes the dentary symphysis's angle as gorgonopsid-like with a strong angular chin. This misunderstanding is probably due to the damage and distortion of the anterior jaw of AMG 4208. In CGP/1/2301, in which the dentary symphysis has been preserved, it is evident that the jaw slopes back gently and does not form a prominent angle. The choanal crests of AMG 4208 appear more pronounced than that of CGP/1/2301.

Cradognathus albanensis is then distinguished from the *Cerdosuchoides–Moschorhinus–Euchambersia* clade by presenting a concave ventral step on the maxillary facial plate, a zygomatic arch which is at its greatest width midway along its length, the upturning of the alveolar margin, a distinct mastoid process, the presence of a diastema between the maxillary canine and first maxillary postcanine, only three lower incisors, a premaxilla which hangs over the incisors forming a pointed snout, a vomer whose anterior extent does not extend beyond the anterior limit of the choanae and the presence of a functional precanine. Only *Cradognathus* displays a zygomatic arch with its greatest width midway along its length within the Therocephalia, apart from the aberrant family Nanictidopidae (*Caodeyao*, *Purlovia*, and *Nanictidops*). A moderate to pronounced upturning of the alveolar margin is also present in *Cerdosuchoides* and *Moschorhinus.* A distinct mastoid process is shared with *Olivierosuchus* and *Promoschorhynchus* and is absent or poorly developed in the other akidnognathids (uncoded for *Shiguaignathus*, *Akidnognathus*, and *Cerdosuchoides*). Only *Cradognathus* and *Annatherapsidus* display just three lower incisors rather than the four of other akidnognathids. *Cradognathus* shares the presence of a maxillary diastema with only *Jiufengia* among the akidnognathids. *Cradognathus* conforms with most of the akidnognathids in having a pointed snout and a vomer whose anterior extent approaches the anterior limit of the choanae differing only with the remaining *Cerdosuchoides–Moschorhinus–Euchambersia* clade with the basal akidnognathids (*Annatherapsidus*, *Shiguaignathus*, and *Jiufengia*) ending more posteriorly. This indicates that despite assumptions by previous authors, the taxon represented by AMG 4208 and CGP/1/2301, renamed *Cradognathus albanensis* herein, is likely not a juvenile *Moschorhinus* (Kitching 1977) and should be retained as a separate taxon, as suggested by Mendrez (1974). This is further supported by the bootstrap values for the *Cerdosuchoides–Moschorhinus–Euchambersia* clade (100).

Conclusions

In conclusion, the above provided description of CGP/1/2301 shows that this specimen is most similar to and very likely represents the same species as AMG 4208, which was previously known as *Hewittia albanensis* Brink, 1959. The genus name has since been found to be preoccupied and so a new name is required. We propose the name *Cradognathus* here. The phylogenetic analysis places *Cradognathus* within a clade that includes *Cerdosuchoides*, *Moschorhinus*, and *Euchambersia*. Due to the relatively good condition of the braincase, it is suggested that a study of the internal anatomy of the skull be undertaken.

Acknowledgements

Thanks to the Blignaut family, Cassie, Herkulien, and Francois (Nxuba, South Africa) for the discovery CGP/1/2301 and for their enthusiastic support which helped to resurrect this little-known species and put it in its rightful place in the ancestral lineage leading to mammals. A further thanks to the following institutions and collection managers who assisted in our visits to their collections: Elize Butler (NMQR); Rose Prevec (AMG); Heidi Fourie (Ditsong Museum of Natural History, Pretoria, South Africa); Cameron Penn-Clarke (CGP); Claire Browning and Zaituna Skosan (SAM); Sifelani Jirah and Bernhard Zipfel (BP); Bruce Rubidge (RC).

Editor: Eli Amson.

References

Abdala, F. 2007. Redescription of *Platycraniellus elegans* (Therapsida, Cynodontia) from the Lower Triassic of South Africa, and the cladistic relationships of eutheriodonts. *Palaeontology* 50: 591–618.

Abdala, F., Gaetano, L.C., Smith, R.M.H., and Rubidge, B.S. 2019. A new large cynodont from the late Permian (Lopingian) of the South African Karoo Basin and its phylogenetic significance. *Zoological Journal of the Linnean Society* 186: 983–1005.

Angielczyk, K.D. and Kammerer, C.F. 2018. Non-Mammalian synapsids: the deep roots of the mammalian family tree. *In*: F. Zachos and R. Asher (eds.), *Mammalian Evolution, Diversity and Systematics*, 117–198. Walter de Gruyter GmbH, Berlin.

Barry, T.H. 1965. On the epipterygoid-alisphenoid transition in Therapsida. *Annals of the South African Museum* 48: 399–426.

Benoit, J., Norton, L.A., Manger, P.R., and Rubidge, B.S. 2017. Reappraisal of the envenoming capacity of *Euchambersia mirabilis* (Therapsida, Therocephalia) using μCT-scanning techniques. *PLoS One* 12 (2): e0172047.

Boonstra, L.D. 1934. A contribution to the morphology of the mammal-like reptiles of the suborder Therocephalia. *Annals of the South African Museum* 31: 215–267.

Botha-Brink, J. and Modesto, S.P. 2011. A new skeleton of the therocephalian synapsid *Olivierosuchus parringtoni* from the Lower Triassic South African Karoo Basin. *Palaeontology* 54: 591–606.

Botha, J., Abdala, F., and Smith, R.M.H. 2007. The oldest cynodont: new clues on the origin and early diversification of the Cynodontia. *Zoological Journal of the Linnean Society* 149: 477–492.

Brink, A.S. 1959. Notes on some whaitsiids and moschorhinids. *Palaeontologica Africana* 6: 23–49.

Brink, A.S. 1963. On *Bauria cynops* Broom. *Palaeontologia Africana* 8: 39–56.

Brink, A.S. 1965. A new ictidosuchid (Scaloposauria) from the *Lystrosaurus*-zone. *Palaeontologica Africana* 9: 129–138.

Brink, A.S. 1988. *Illustrated Bibliographical Catalogue of the Synapsida, Part 2*. 350 pp. Geological Survey of South Africa, Pretoria.

Broom, R. 1936. On some new genera and species of Karroo fossil reptiles, with notes on some others. *Annals of the Transvaal Museum* 18: 349–386.

de Lessert, R. 1928. Araignees du Congo. *Revue Suisse de Zoologie* 35 (18): 303–352.

Durand, J.F. 1989. *Aspects of the Cranial Morphology of the Therocephalian* Moschorhinus *(Reptilia: Therapsida)*. 210 pp. University of Witwatersrand, Johannesburg.

Durand, J.F. 1991. A revised description of the skull of *Moschorhinus* (Therapsida, Therocephalia). *Annals of the South African Museum* 99 (2): 381–413.

Gigliotti, A., Pusch, L.C., Kammerer, C.F., Benoit, J., and Fröbisch, J. 2023. Craniomandibular anatomy of the akidnognathid therocephalian *Olivierosuchus parringtoni* from the Early Triassic of South Africa. *Palaeontologia Africana* 56: 142–170.

Grunert, H.R., Brocklehurst, N., and Fröbisch, J. 2019. Diversity and disparity of Therocephalia: macroevolutionary patterns through two mass extinctions. *Scientific Reports* 9: 5063–5075.

Haughton, S.H. 1918. Investigations in South African fossil reptiles and Amphibia (Part 2). *Annals of the South African Museum* 12 (6): 175–216.

Hopson, J.A. and Barghusen, H. 1986. An analysis of therapsid relationships. *In*: N. Hotton, P.D. MacLean, J.J. Roth, and E.C. Roth (eds.), *The Ecology and Biology of Mammal-like Reptiles*, 83–106. Smithsonian Institution Press, Washington.

Huttenlocker, A. 2009. An investigation into the cladistic relationships and monophyly of therocephalian therapsids (Amniota: Synapsida). *Zoological Journal of the Linnean Society* 157: 865–891.

Huttenlocker, A.K. 2013. *The Paleobiology of South African Therocephalian Therapsids (Amniota, Synapsida) and the Effects of the End-Permian Extinction on Size, Growth, and Bone Microstructure*. 414 pp. Unpublished Ph.D. dissertation, University of Washington, Seattle.

Huttenlocker, A.K. 2014. Body size reductions in nonmammalian eutheriodont therapsids (Synapsida) during the end-Permian mass extinction. *PLoS One* 9 (2): e87553.

Huttenlocker, A.K. and Abdala, F. 2015. Revision of the first therocephalian, *Theriognathus* Owen (Therapsida: Whaitsiidae), and implications for cranial ontogeny and allometry in nonmammaliaform eutheriodonts. *Journal of Paleontology* 89 (4): 645–664.

Huttenlocker, A.K. and Botha-Brink, J. 2013. Body size and growth patterns in the therocephalian *Moschorhinus kitchingi* (Therapsida: Eutheriodontia) before and after the end-Permian extinction in South Africa. *Paleobiology* 39: 253–277.

Huttenlocker, A.K. and Sidor, C.A. 2012. Taxonomic revision of therocephalians (Therapsida: Theriodontia) from the Lower Triassic of Antarctica. *American Museum Novitates* 3738: 19.

Huttenlocker, A.K. and Sidor, C.A. 2020. A basal nonmammaliaform cynodont from the Permian of Zambia and the origins of mammalian endocranial and postcranial anatomy. *Journal of Vertebrate Paleontology* 40 (5): e1827413.

Huttenlocker, A.K. and Smith, R.M.H. 2017. New whaitsioids (Therapsida: Therocephalia) from the Teekloof Formation of South Africa and therocephalian diversity during the end-Guadalupian extinction. *PeerJ* 5: e3868.

Huttenlocker, A.K., Sidor, C.A., and Smith, R.M.H. 2011. A new specimen of *Promoschorhynchus* (Therapsida: Therocephalia: Akidnognathidae) from the Lower Triassic of South Africa and its implications for theriodont survivorship across the Permo–Triassic boundary. *Journal of Vertebrate Paleontology* 31: 405–421.

Kemp, T.S. 1972. Whaitsiid Therocephalia and the origin of cynodonts. *Philosophical Transactions of the Royal Society of London, Series B* 264: 1–54.

Kemp, T.S. 2005. *The Origin and Evolution of Mammals*. 331 pp. Oxford University Press, Oxford.

Kitching, J.W. 1977. *The Distribution of the Karroo Vertebrate Fauna. Memoir 1*. 131 pp. Bernard Price Institute for Palaeontological Research, University of the Witwatersrand, Johannesburg.

Liu, J. and Abdala, F. 2017. The tetrapod fauna of the upper Permian Naobaogou Formation of China: 1. *Shiguaignathus wangi* gen. et sp. nov., the first akidnognathid therocephalian from China. *PeerJ* 5: e4150.

Liu, J. and Abdala, F. 2019. The tetrapod fauna of the upper Permian Naobaogou Formation of China: 3. *Jiufengia jiai* gen. et sp. nov., a large akidnognathid therocephalian. *PeerJ* 7: e6463.

Liu, J. and Abdala, F. 2020. The tetrapod fauna of the upper Permian Naobaogou Formation of China: 5. *Caodeyao liuyufengi* gen. et sp. nov., a new peculiar therocephalian. *PeerJ* 8: e9160.

Liu, J. and Abdala, F. 2022. The emblematic South African therocephalian *Euchambersia* in China: a new link in the dispersal of late Permian vertebrates across Pangea. *Biology Letters* 18: 20220222.

Maier, W., Van Den Heever, J., and Durand, J. 1996. New therapsid specimens and the origin of the secondary hard and soft palate. *Journal of Zoological Systematics and Evolutionary Research* 34: 9–19.

Mendrez, C.H. 1974. A new specimen of *Promoschorhynchus platyrhinus* Brink 1954 (Moschorhinidae) from the *Daptocephalus*-zone (upper Permian) of South Africa. *Palaeontologia Africana* 17: 69–85.

Pusch, L.C., Kammerer, C.F., and Fröbisch, J. 2019. Cranial anatomy of the early cynodont *Galesaurus planiceps* and the origin of mammalian endocranial characters. *Journal of Anatomy* 234: 592–621.

Pusch, L.C., Kammerer, C.F., and Fröbisch, J. 2021. Cranial anatomy of *Bolotridon frerensis*, an enigmatic cynodont from the Middle Triassic of South Africa, and its phylogenetic significance. *PeerJ* 9: e11542.

Pusch, L.C., Kammerer, C.F., and Fröbisch, J. 2024. The origin and evolution of Cynodontia (Synapsida, Therapsida): Reassessment of the phylogeny and systematics of the earliest members of this clade using 3D-imaging technologies. *The Anatomical Record* 307: 1634–1730.

Pusch, L.C., Ponstein, J., Kammerer, C.F., and Fröbisch, J. 2020. Novel endocranial data on the early therocephalian *Lycosuchus vanderrieti* underpin high character variability in early theriodont evolution. *Frontiers in Ecology and Evolution* 7: 464.

Pusch, L.C., Kammerer, C.F., Fernandez, V., and Fröbisch, J. 2023. Cranial anatomy of *Nythosaurus larvatus* Owen, 1876, an Early Triassic cynodont preserving a natural endocast. *Journal of Vertebrate Paleontology* 42 (1): e2174441.

Rubidge, B.S. and Sidor, C.A. 2001. Evolutionary patterns among Permo-Triassic therapsids. *Annual Review of Ecology and Systematics* 32: 449–480.

Sidor, C.A., Kulik, Z.T., and Huttenlocker, A.K. 2021. A new bauriamorph therocephalian adds a novel component to the Lower Triassic tetrapod assemblage of the Fremouw Formation (Transantarctic Basin) of Antarctica. *Journal of Vertebrate Paleontology* 41 (6): e2081510.

Sigurdsen, T., Huttenlocker, A.K., Modesto, S.P., Rowe, T.B., and Damiani, R. 2012. Reassessment of the morphology and paleobiology of the therocephalian *Tetracynodon darti* (Therapsida), and the phylogenetic relationships of Baurioidea. *Journal of Vertebrate Paleontology* 32: 1113–1134.

Smith, R.M.H., Rubidge, B.S., Day, M.O., and Botha, J. 2020. Introduction to the tetrapod biozonation of the Karoo Supergroup. *South African Journal of Geology* 123: 131–140.

Swofford, D.L. 2002. *PAUP. Phylogenetic Analysis Using Parsimony (and Other Methods), Version 4.* Sinauer Associates, Sunderland.

Van Den Heever, J.A. 1994. The cranial anatomy of the early Therocephalia (Amniota: Therapsida) *Annals of the University of Stellenbosch* 1: 1–59.

Viglietti, P.A. 2020. Biostratigraphy of the *Daptocephalus* Assemblage Zone (Beaufort Group, Karoo Supergroup), South Africa. *South African Journal of Geology* 123: 191–206.

Viglietti, P.A., Benson, R.B.J., Smith, R.M.H., Botha, J., Kammerer, C.F., Skosan, Z., Butler, E., Crean, A., Eloff, B., Kaal, S., Mohoi, J., Molehe, W., Mtalana, N., Mtungata, S., Ntheri, N., Ntsala, T., Nyaphuli, J., October, P., Skinner, G., Strong, M., Stummer, H., Wolvaardt, F., and Angielczyk, K.D. 2021. Evidence from South Africa for a protracted end-Permian extinction on land. *PNAS* 118 (17): e2017045118.